Three-Dimensionally Arranged Windmill and Grid Porphyrin Arrays by Ag^{I}-Promoted *meso*–*meso* Block Oligomerization

Aiko Nakano,[a] Tomoko Yamazaki,[b] Yoshinobu Nishimura,[b] Iwao Yamazaki,[b] and Atsuhiro Osuka*[a]

Abstract: The syntheses of soluble windmill and grid porphyrin arrays through the Ag^{I}-promoted coupling reaction of 1,4-phenylene-bridged linear porphyrin arrays, which are comprised of a central Zn^{II} β-free porphyrin and flanking peripheral Ni^{II} β-octaalkylporphyrins, are described. The coupling reaction is advantageous in light of its high regioselectivity occurring only at the *meso*-position of the Zn^{II} β-free porphyrin as well as its easy extension to large porphyrin arrays. The windmill porphyrin arrays in turn serve as an effective substrate for further coupling reactions, to give three-dimensionally arranged grid porphyrin arrays. Further the grid porphyrin 12-mer (a tetramer of the linear porphyrin trimer) was also coupled to afford grid porphyrins (24-mer, 36-mer, and 48-mer). These porphyrin arrays were isolated in a discrete form by repetitive GPC/HPLC (GPC = gel-permiation chromatography). Competitive experiments with three linear porphyrin trimers bearing different peripheral metalloporphyrins (Zn^{II}, Ni^{II}, and Cu^{II}), and the trapping experiment of the radical cation at the peripheral porphyrin with $AgNO_2$, suggested that an initial one-electron oxidation of the easily oxidizable peripheral Zn^{II} β-octaalkylporphyrin with an Ag^{I} ion and a subsequent endothermic hole transfer assist the generation of the radical cation at the central Zn^{II} β-free porphyrin. In all Zn^{II}-metallated windmill porphyrin arrays, the energy level of the S_1 state of the *meso*–*meso*-linked diporphyrin core is lower than that of the peripheral porphyrins, thereby allowing an energy flow from the peripheral porphyrins to the central diporphyrin core; this has been confirmed by measurements of fluorescence lifetimes and picosecond time-resolved fluorescence spectra. The excitation energy transfer in the arrays encourages their potential use as an light-harvesting antenna.

Keywords: oligomerizations · oligomers · photochemistry · porphyrinoids · transition metals

Introduction

The design and construction of novel porphyrin architectures with well-defined geometries is an area of increasing current interest.[1] These porphyrin assemblies are of fundamental importance as attractive building blocks for the modular construction of electronics, optical devices, sensors, and solar energy conversion.[2, 3, 4] A number of covalently linked or noncovalently assembled porphyrin arrays have been developed with the aim of reproducing and understanding light-harvesting and charge-separation phenomena in photosynthetic organisms.[5, 6] In view of higher stability and better tunability of electronic interactions between an energy donor and an energy acceptor, the covalent-linkage strategy has offered far more promise for the construction of a robust molecular system and for probing the effects of molecular organization on electronic interactions necessary for energy transfer processes; this has greatly contributed to our understanding of the natural light-harvesting processes at a molecular level. As a result, a variety of covalently linked porphyrin arrays have been developed; these include linear,[4, 7, 8] cyclic,[9, 10] dendritic,[11] stacked,[12] starburst,[13] bandanna,[14] fused,[15] and other fascinating three-dimensional arrangements.[16, 17, 18] A drawback in the covalent-linkage strategy lies in their time-consuming multi-step syntheses, which become increasingly serious for the synthesis of higher order arrays of porphyrin chromophores; this has stimulated a continuing demand for an effective yet simple synthetic method that can afford large porphyrin arrays with a well-defined arrangement.

Here we report synthesis of three-dimensionally arranged windmill- and grid-like porphyrin arrays. This is an extension

[a] Prof. A. Osuka, A. Nakano
Department of Chemistry, Graduate School of Science
Kyoto University, Sakyo-ku, Kyoto 606-8502 (Japan)
Fax: (+81) 75-753-3970
E-mail: osuka@kuchem.kyoto-u.ac.jp

[b] T. Yamazaki, Y. Nishimura, Prof. I. Yamazaki
Department of Chemical Process Engineering
Graduate School of Engineering, Hokkaido University
Sapporo 060-8628 (Japan)

  0947-6539/00/0617-3254 $ 17.50+.50/0

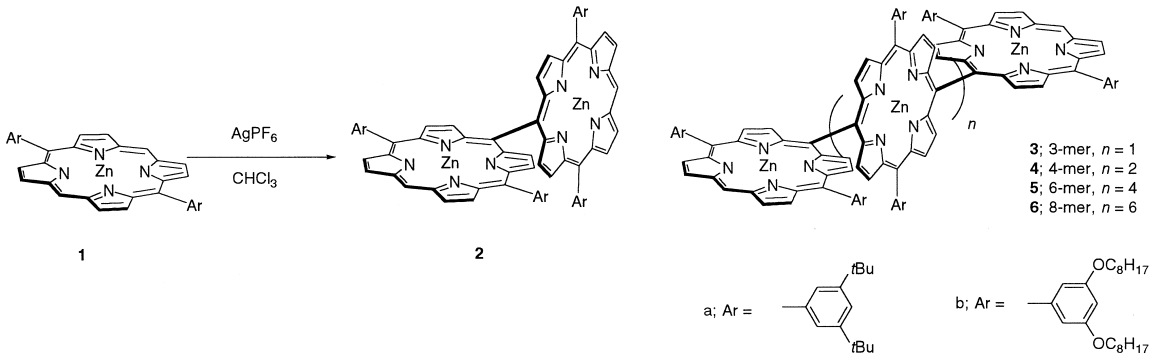

Scheme 1. *meso*–*meso*-Coupling reaction of Zn^{II} 5,15-diarylporphyrin.

of our recent synthesis of *meso*–*meso*-linked porphyrin oligomers from a Zn^{II} 5,15-diarylporphyrin with an Ag^{I} ion in $CHCl_3$.[17] As shown in Scheme 1, the treatment of Zn^{II} 5,15-diarylporphyrin **1** with an Ag^{I} ion led to formation of *meso*–*meso*-linked oligomers **2**–**6**. This reaction can be accounted for in terms of initial one-electron oxidation of the Zn^{II} porphyrin with the Ag^{I} ion, followed by nucleophilic attack of a neutral Zn^{II} porphyrin. This mechanism is supported by the synthesis of the same porphyrin oligomers by anodic electrochemical oxidation.[17c,d] If this Ag^{I}-promoted *meso*–*meso*-coupling reaction can be applied to 1,4-phenylene-bridged linear porphyrin arrays with similar high regioselectivity, it would constitute an efficient synthetic entry into a new class of large, three-dimensionally arranged porphyrin arrays. To test this idea we examined the Ag^{I}-promoted reaction of 1,4-phenylene-bridged linear porphyrin arrays that have a reactive Zn^{II} 5,15-diaryl-substituted β-free porphyrin flanked by Ni^{II} β-octaalkylporphyrins. As described below, the *meso*–*meso*-coupling reaction of the linear porphyrin arrays proceeded easily, and resulted in an efficient construction of windmill-like porphyrin arrays.[19] Further we found that the similar coupling reaction of the windmill-like porphyrin arrays led to higher order arrays with three-dimensional grid-like architectures. This synthetic approach is outlined in Scheme 2. Here we call *meso*–*meso*-linked dimer of linear porphyrin array as a "windmill porphyrin array", and its *meso*–*meso*-coupled higher oligomer as a "grid porphyrin array". Three-dimensional grid-like arrangements of metals have attracted considerable interests from a viewpoint of construction of information storage devices.[20] We also report efficient intramolecular singlet–singlet energy transfer from the peripheral porphyrins to the *meso*–*meso*-linked diporphyrin core in all Zn^{II}-metallated windmill porphyrin arrays; this is also of interest with a view to the construction of artificial light-harvesting antenna.

Results and Discussion

Synthesis of windmill porphyrin arrays: For the first step, we examined the Ag^{I}-promoted coupling reaction of the 1,4-phenylene-bridged hybrid porphyrin dimer **10-Ni**, which was prepared by condensation of formyl-substituted porphyrin **7-Ni**[21] and 3,5-di-*tert*-butylbenzaldehyde **9**[22] with 2,2′-dipyrrylmethane **8**[23] using Lindsey conditions[7d, 24] in 12% yield. (Scheme 3). Treatment of **10-Ni** with 1.2 equivalents of $AgPF_6$ at room temperature in $CHCl_3$ followed by separation by gel-permeation chromatography (GPC) gave porphyrin tetramer **11-Ni** in 51% yield, along with recovery of **10-Ni** (33%). The MALDI-TOF MS spectrum of **11-Ni** displayed a parent ion peak at *m*/*z* 3243 (calcd for $C_{206}H_{230}N_{16}Ni_2O_4Zn_2$: 3242); the ^1H NMR spectrum displayed a singlet due to the *meso* protons of Zn^{II} β-free porphyrin at $\delta = 10.53$ and broad signals for the *meso* protons of Ni^{II} β-octaalkylporphyrin at $\delta = 9.53$ and 9.37,

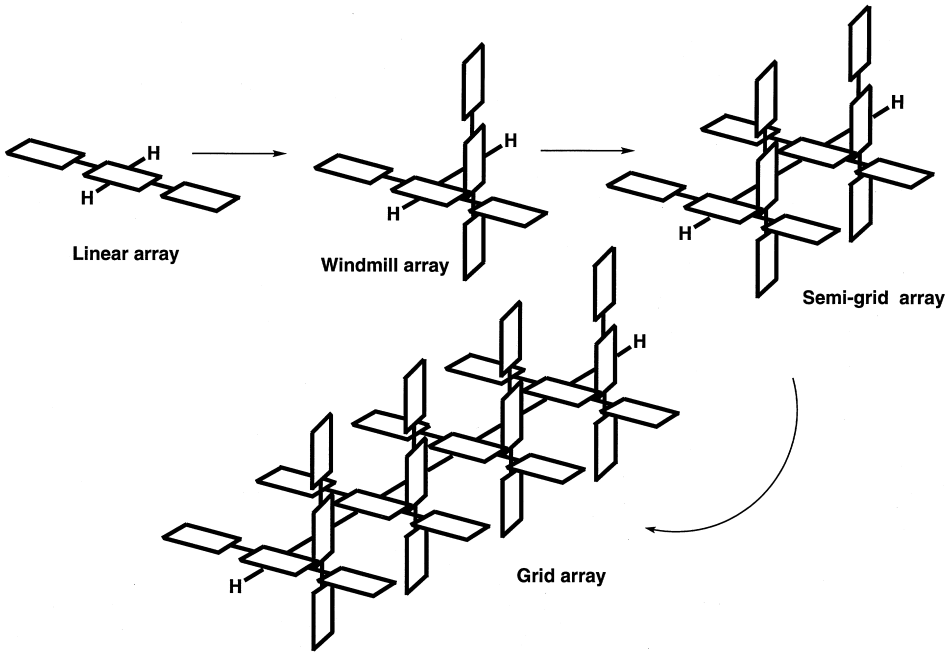

Scheme 2. Synthetic scheme of windmill and grid porphyrin arrays.

  0947-6539/00/0617-3255 $ 17.50+.50/0

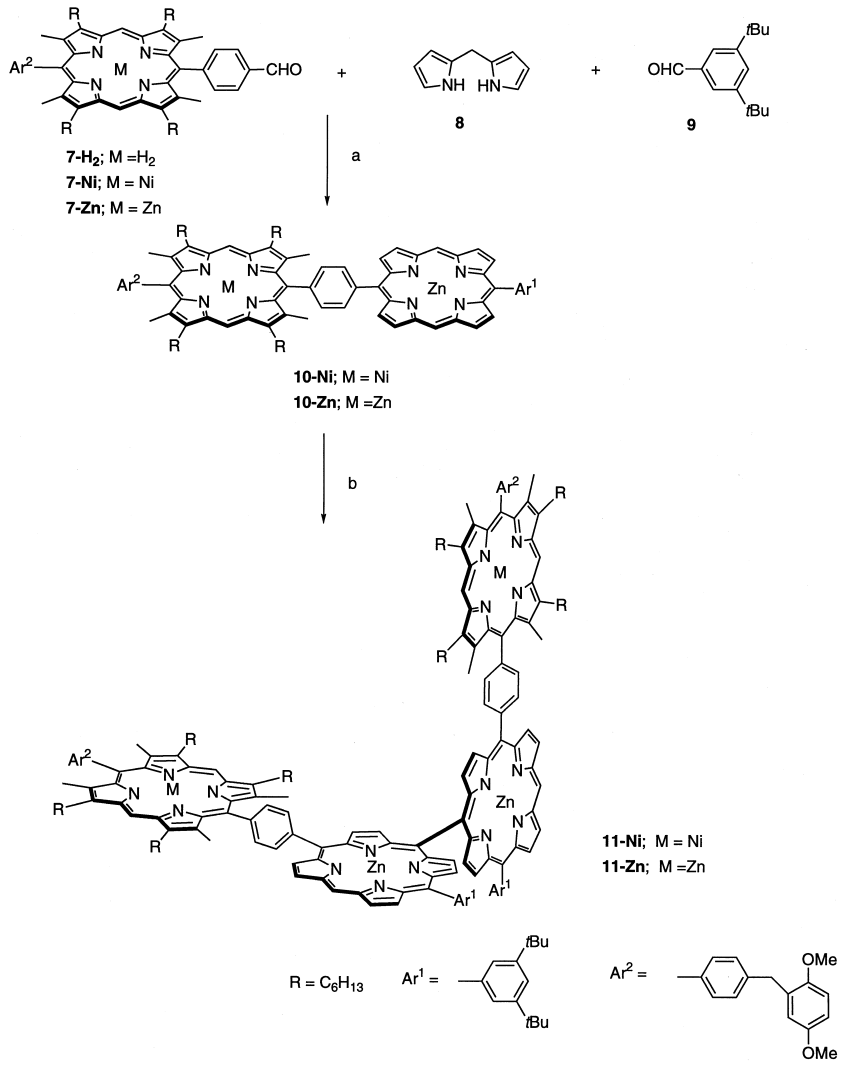

Scheme 3. Synthesis of porphyrin tetramers **11-Ni** and **11-Zn**; a) TFA, CH_2Cl_2; *p*-chloranil; $Zn(OAc)_2$. b) $AgPF_6$, $CHCl_3$.

as well as for the eight β protons of the Zn^{II} β-free porphyrin at $\delta = 9.71$, 9.59, 9.53, 9.26, 9.10, 8.83, 8.39, and 8.26, which are characteristic of the *meso*–*meso*-linked porphyrin dimer.[17] Similar reaction of **10-Zn** led to formation of **11-Zn** only in 5% yield along with 40% recovery. The one-electron oxidation potentials of **1a**, **7-Zn**, and **7-Ni** in $CHCl_3$, measured by cyclic voltammetry, were found to be 0.30, 0.17, and 0.32 V, respectively, versus a ferrocene/ferrocenium ion couple. Since the oxidation reactions of the Ni^{II} β-octaalkylporphyrin and the Zn^{II} β-free porphyrin by an Ag^{I} ion have similar endothermicity, the radical cation of Zn^{II} β-free porphyrin in **10-Ni** may be generated, in addition to direct oxidation of the Zn^{II} β-free porphyrin by an Ag^{I} ion, through an indirect route that involves initial oxidation of the Ni^{II} β-octaalkylporphyrin with the Ag^{I} ion, followed by hole transfer. The observed low yield of **11-Zn** suggested undesirable side reactions of the peripheral Zn^{II} β-octaalkylporphyrin radical cation. Based on these results, we employed Ni^{II} β-octaalkylporphyrin as a peripheral-protecting unit.

As the next step, we examined the Ag^{I}-promoted coupling reaction of 1,4-phenylene-bridged linear porphyrin arrays such as trimer **14-Ni**, pentamer **15-Ni**, and heptamer **16-Ni**. Synthesis of 1,4-phenylene-bridged linear porphyrin arrays have been previously reported by us[7a,b] and Sessler.[7c,d] Thus, the target linear porphyrin arrays **14-Ni**, **15-Ni**, and **16-Ni** were prepared by a similar route with replacement of a β-alkyl-substituted dipyrrylmethane by β-unsubstituted dipyrrylmethane **8**. Symmetric linear porphyrin trimer **14-Ni** (51% yield), pentamer **15-Ni** (68% yield), and heptamer **16-Ni** (80% yield) were prepared from corresponding Ni^{II} formyl-substituted porphyrin monomer **7-Ni**, dimer **12-Ni** and trimer **13-Ni**, respectively (TFA, CH_2Cl_2; *p*-chloranil). High yields of these 1,4-phenylene-bridged linear porphyrin arrays are worthy to note.

The reaction of the trimer **14-Ni** with two equivalents of $AgPF_6$ produced porphyrin hexamer **17-Ni** along with porphyrin nonamer **18** as monitored by analytical GPC/HPLC (Figure 1b, left). The reaction was stopped after 22 h and **17-Ni** and **18** were isolated by recycling preparative GPC/HPLC in 50% and 2% yields (Figure 1c and 1d, left), respectively, along with the recovery of **14-Ni** (47%) (Scheme 4). The molecular weights of these porphyrin arrays were determined by MALDI-TOF MS: **17-Ni** *m*/*z* 4985 (calcd for $C_{316}H_{358}N_{24}Ni_4O_8Zn_2$: 4985) and **18** *m*/*z* 7476 (calcd for $C_{474}H_{536}N_{36}Ni_6O_{12}Zn_3$: 7478). The 500 MHz ^1H NMR spectra of **14-Ni**, **17-Ni**, and **18** shown in Figure 2 display well-resolved and relatively simple patterns in spite of their large molecular sizes. Orthogonal architecture of these arrays, which prevents $\pi-\pi$ stacking may lead to the well-resolved ^1H NMR spectra, and their symmetric structures are consistent with the simple ^1H NMR spectra. Singlet signals for the *meso* protons in the central *meso*–*meso*-linked porphyrins (H^a, indicated by open arrows in Figure 2) of both **17-Ni** and **18** appeared at nearly the same chemical shift as that of **14-Ni**, and the chemical shifts of the β-protons are analogous to those of **1**, **2**, and **3**,[17] and appear at $\delta = 9.68$ (H^c) and 9.53 (H^d) in **14-Ni**, at $\delta = 9.79$ (H^c), 9.60 (H^d), 9.18 (H^e), and 8.52 (H^f) in **17-Ni**, and at $\delta =$ 9.82 (H^c), 9.64 (H^d), 9.34 (H^e), 9.26 (H^h), 8.76 (H^f), and 8.65 (H^g) in **18**. By using the ROESY ^1H NMR technique, all the signals in the aromatic region of **17-Ni** and **18** were fully assigned as shown in Figure 2 (designations are given in

  0947-6539/00/0617-3256 $ 17.50+.50/0 *Chem. Eur. J.* **2000**, *6*, No. 17

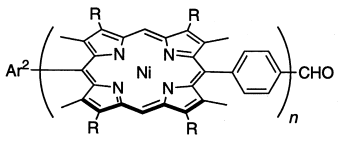

7-Ni; $n = 1$
12-Ni; $n = 2$
13-Ni; $n = 3$

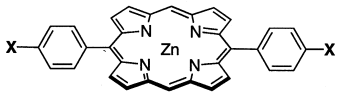

14-Ni; X = P(Ni), 3-mer
14-Zn; X = P(Zn), 3-mer
15-Ni; X = PP(Ni), 5-mer
15-Zn; X = PP(Zn), 5-mer
16-Ni; X = PPP, 7-mer

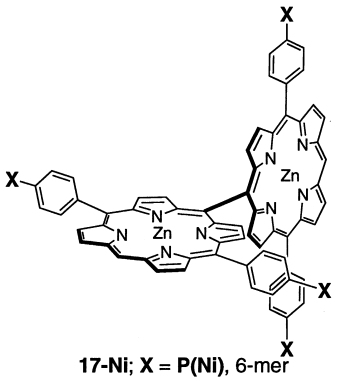

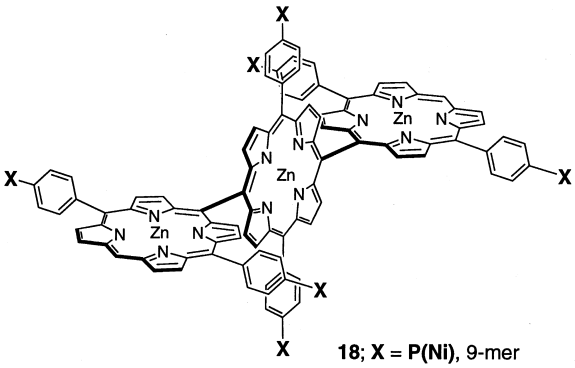

18; X = P(Ni), 9-mer
20; X = PP(Ni), 15-mer

17-Ni; X = P(Ni), 6-mer
17-Zn; X = P(Zn), 6-mer
19-Ni; X = PP(Ni), 10-mer
19-Zn; X = PP(Zn), 10-mer
21-Ni; X = PPP, 14-mer

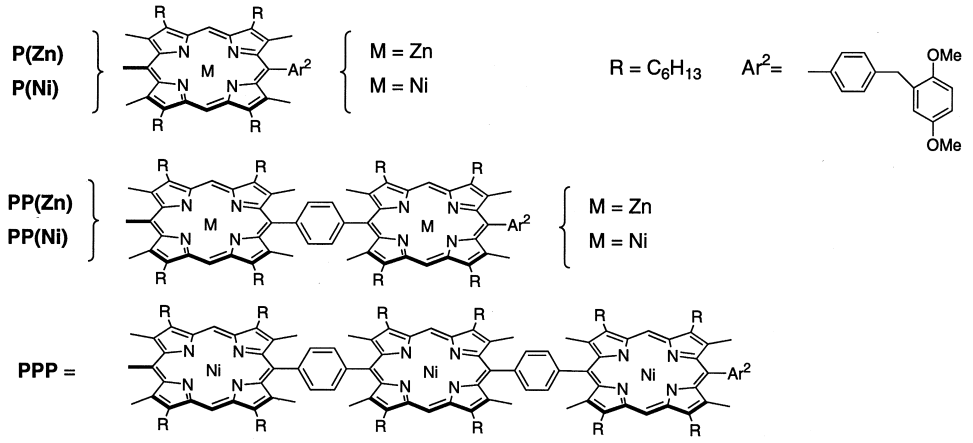

Scheme 4). An interesting feature is that the two *meso* protons and the β-methyl protons at the peripheral β-octaalkylporphyrin were observed separately in the ^{1}H NMR spectra of both **17-Ni** and **18**; the *meso* protons H^b and $H^{b'}$ in the peripheral porphyrins appeared at $\delta = 9.53$ and 9.36, and the peripheral β-methyl protons appeared at $\delta = 2.96$ (12H), 2.58 (12H), and 2.23 (24H) ppm in **17-Ni**. These observations suggested restricted rotation around C–C bond between the *meso* carbon at the central β-free porphyrin and the 1,4-phenylene spacer. As shown in Figure 3, the ^{1}H NMR spectrum of **17-Ni** was temperature dependent, and the *meso* protons H^b and $H^{b'}$ appeared as two singlets at $\delta = 9.52$ and 9.35 at $-30\,^\circ$C and changed to a broad signal at $\delta = 9.46$ at $50\,^\circ$C in $CDCl_3$. In the ^{1}H NMR spectrum of **18**, $H^{b''}$ of the peripheral Ni^{II} β-octaalkylporphyrins in the inner array appeared as a singlet at $\delta = 9.33$ and H^b and $H^{b'}$ appeared as two separate broad signals at $\delta = 9.56$ and 9.41, similar to those in **17-Ni** (Figure 2c). On the basis of the variable temperature ^{1}H NMR measurements, the activation barrier of the rotation of the peripheral porphyrin has been estimated to be 15.5–16 kcal mol^{-1} for **17-Ni**.

The coupling reaction of the linear porphyrin pentamer **15-Ni** was similarly performed with three equivalents of $AgPF_6$. Monitoring by analytical GPC/HPLC (Figure 1b, middle) revealed the appearance of new bands eluting at 18.9 and 18.1 min; these were assigned to porphyrin decamer **19-Ni** and

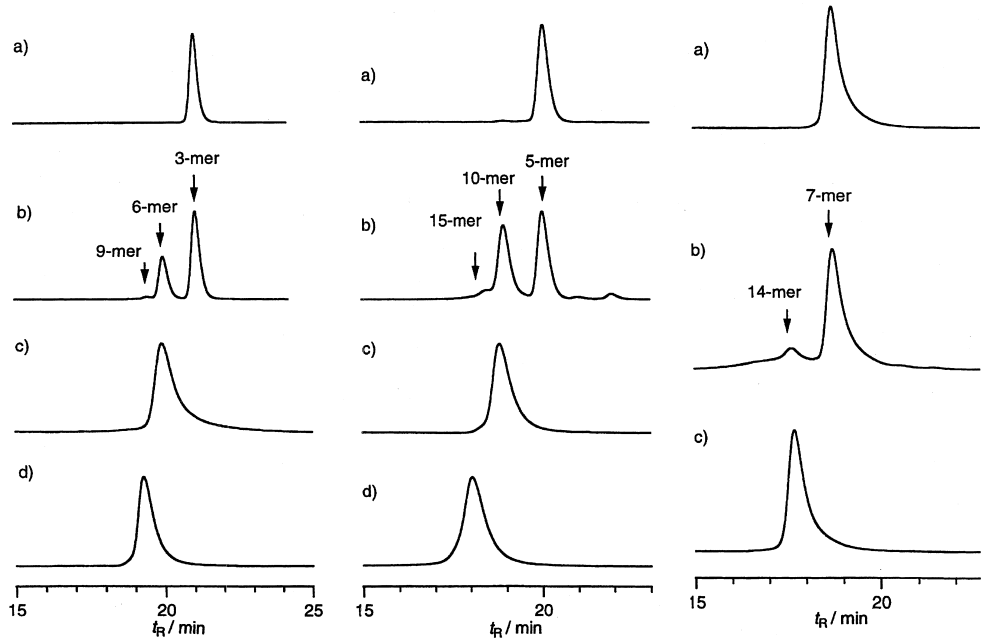

Figure 1. GPC/HPLC chromatograms of the Ag^I-promoted coupling reaction detected at 420 nm. Each chromatogram is normalized to the maximum intensity. Left: the reaction of **14-Ni**: a) **14-Ni**, b) after 12 h, c) purified **17-Ni**, and d) purified **18**. Middle: the reaction of **15-Ni**: a) **15-Ni**, b) after 12 h, c) purified **19-Ni**, and d) purified **20**. Right: the reaction of **16-Ni**: a) **16-Ni**, b) after 16 h, and c) purified **21-Ni**.

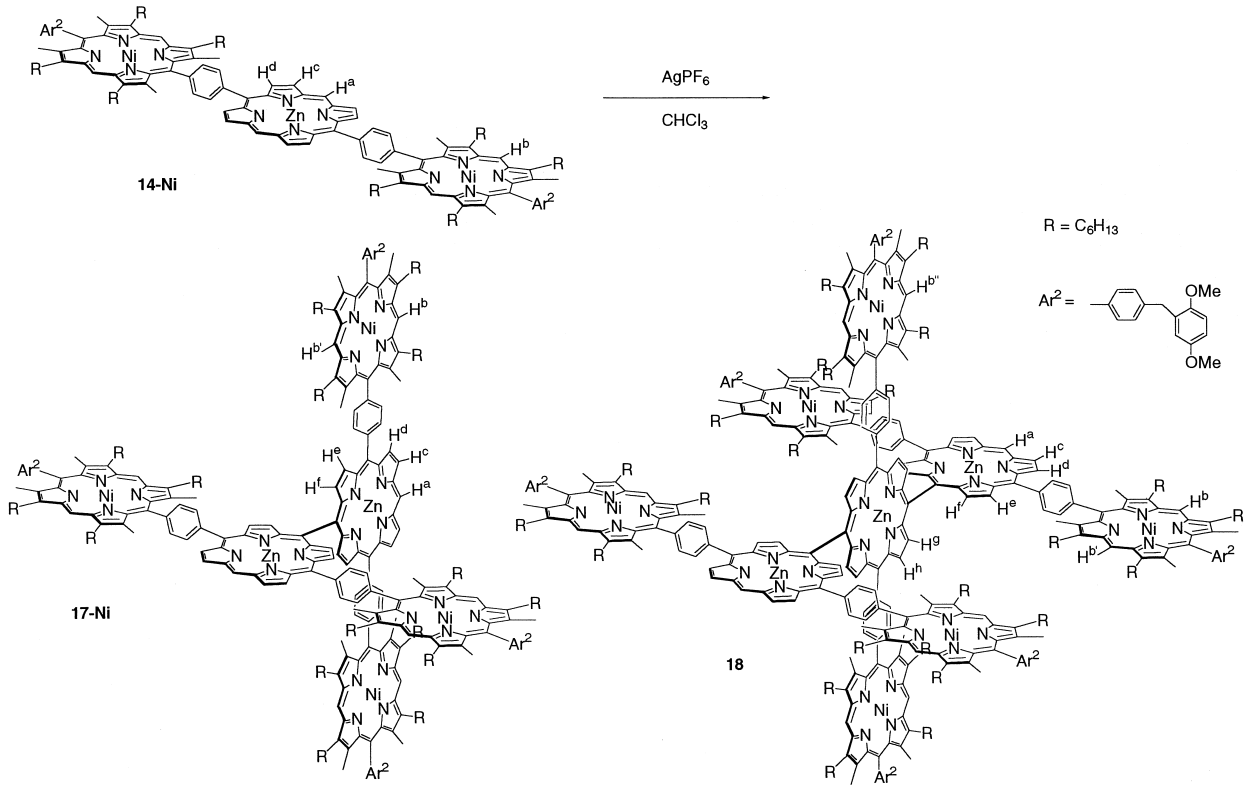

Scheme 4. Synthesis of windmill hexamer.

porphyrin 15-mer **20**, respectively. The reaction was stopped after 25 h and the separation by recycling preparative GPC/HPLC gave porphyrin decamer **19-Ni** (35% isolated yield, MALDI-TOF MS: *m*/*z* 8321; calcd for $C_{532}H_{638}N_{40}Ni_8O_8Zn_2$: 8320, Figure 1c middle). The decamer **19-Ni** displayed a well-resolved ^1H NMR spectrum, which was fully consistent with the assigned windmill structure. Further the reaction of the porphyrin heptamer **16-Ni** with three equivalents of $AgPF_6$ also provided porphyrin 14-mer **21-Ni** (MALDI-TOF MS: *m*/*z* 11640; calcd for $C_{748}H_{918}N_{56}Ni_{12}O_8Zn_2$: 11656) with a 14% isolated yield (Figure 1, right). The yields are summarized in Table 1.

0947-6539/00/0617-3258 $ 17.50+.50/0 *Chem. Eur. J.* **2000**, *6*, No. 17

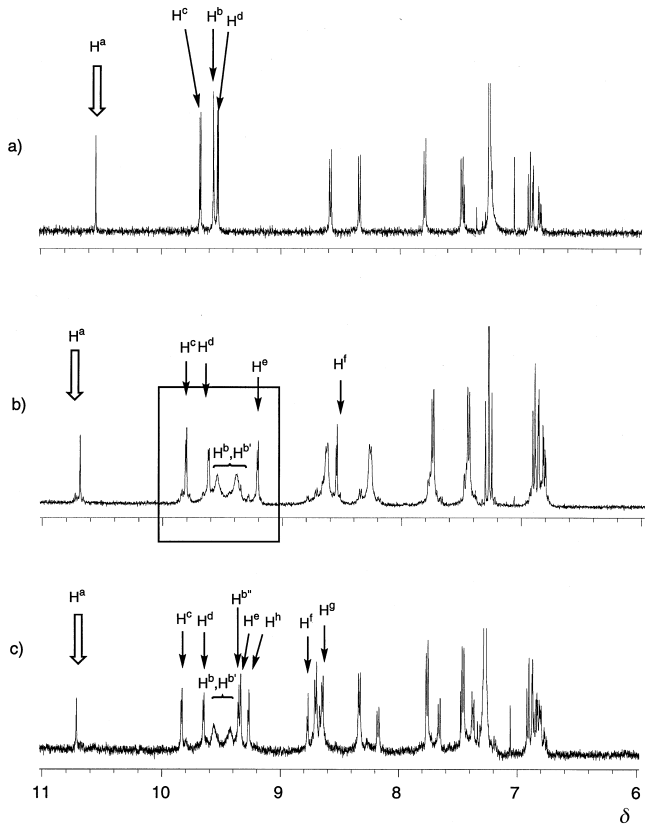

Figure 2. ^{1}H NMR spectra a) **14-Ni**, b) **17-Ni**, and c) **18** in $CDCl_3$. Designation of the protons is given in Scheme 4.

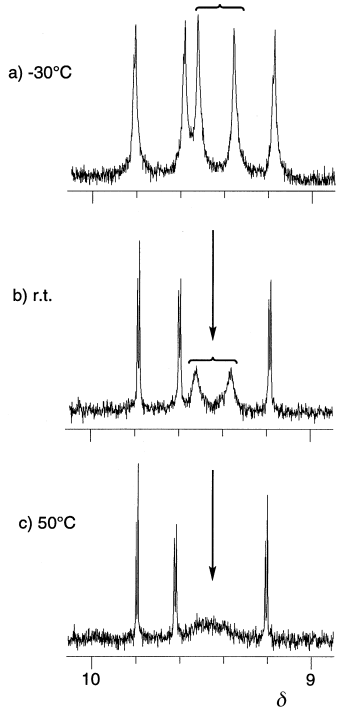

Figure 3. ^{1}H NMR spectra of **17-Ni** at variable temperature: a) at −30 °C, b) room temperature, and c) at 50 °C in $CDCl_3$.

Synthesis of grid porphyrin arrays: As indicated above, the coupling reaction of the linear porphyrin arrays often led to production of higher oligomerized porphyrin arrays such as the nonamer **18** and the 15-mer **20**. These results suggested that windmill porphyrins themselves could serve as an effective building block for the Ag^I-promoted coupling reaction. Therefore, we examined Ag^I-promoted coupling reaction of the windmill porphyrin arrays. In these attempts, we employed substrates **24-Ni** (porphyrin trimer) and **32** (porphyrin pentamer) bearing 3,5-dioctyloxyphenyl substituents as starting linear porphyrin arrays in order to improve solubilities of higher oligomeric porphyrin products. The trimer **24-Ni** and the pentamer **32** were prepared by a similar route used for preparation of **14-Ni** and **15-Ni**.

Windmill porphyrin hexamer **25-Ni** (MALDI-TOF MS, *m*/*z* 5400; calcd for $C_{344}H_{446}N_{24}Ni_4O_8Zn_2$: 5411) and windmill decamer **33** (MALDI-TOF MS, *m*/*z* 8741; calcd for $C_{560}H_{726}N_{40}Ni_8O_8Zn_2$: 8746) were prepared from **24-Ni** and **32** in 22 % and 28 % yields, respectively. The reaction of **25-Ni** with two equivalents $AgPF_6$ for 9 h gave a mixture that contained porphyrin 12-mer **27**, 18-mer **28**, and 24-mer **29** as monitored by the analytical GPC/HPLC (Figure 4a, left); these were separated by recycling preparative GPC/HPLC to give the 12-mer **27** (25 %) (Figure 4b, left) and small amounts of the 18-mer **28** and the 24-mer **29** along with the recovery of **25-Ni** (35 %). The MALDI-TOF MS measurements revealed that the molecular weights of porphyrin arrays **27** (*m*/*z* 10822; calcd for $C_{688}H_{890}N_{48}Ni_8O_{16}Zn_4$: 10820), **28** (*m*/*z* 16211; calcd for $C_{1032}H_{1334}N_{72}Ni_{12}O_{24}Zn_6$: 16229), and **29** (*m*/*z* 21466; calcd for $C_{1376}H_{1778}N_{96}Ni_{16}O_{32}Zn_8$: 21638) are in excellent agreement with the assigned structures. The windmill 10-mer **33** was treated under the similar conditions (Figure 4c, right), and the porphyrin oligomers were separated by recycling preparative GPC/HPLC. The molecular weight of the product that eluted at 17.4 min (Figure 4d, right) was determined by MALDI-TOF MS to be *m*/*z* 17426, and this

Table 1. Results of Ag^I-promoted coupling reaction of porphyrin arrays.[a]

Starting compound[b]	Conditions		Results	
	$AgPF_6$ [equiv]	reaction time [h]	recovery [%][c]	product distribution[d]
10-Ni (2)	1.2	11	33	**11-Ni** (51 %)
14-Ni (3)	2.0	21.5	47	**17-Ni** (50 %), **18** (ca. 2 %)
15-Ni (5)	3.1	25	15	**19-Ni** (35 %), **20** (trace)
16-Ni (7)	3.0	16	–	**21-Ni** (14 %)
24-Ni (3)	2.0	24	62	**25-Ni** (22 %), **26-Ni** (trace)
25-Ni (6)	2.0	9	35	**27** (25 %), **28** (trace), **29** (trace)
32 (5)	3.0	6	11	**33** (28 %), **34** (7 %), **35** (trace)
24-Zn (3)	2.0	24	42	**25-Zn** (48 %), **26-Zn** (ca. 3 %)
24-Cu (3)	2.0	20	32	**25-Cu** (46 %), **26-Cu** (8 %)

[a] Reactions were carried out in $CHCl_3$ at room temperature. See the Experimental Section for details. [b] Number in the parentheses indicates the number of the porphyrins in the array. [c] Isolated yield of the recovered starting compound after preparative GPC/HPLC. [d] Isolated yield of the products after preparative GPC/HPLC.

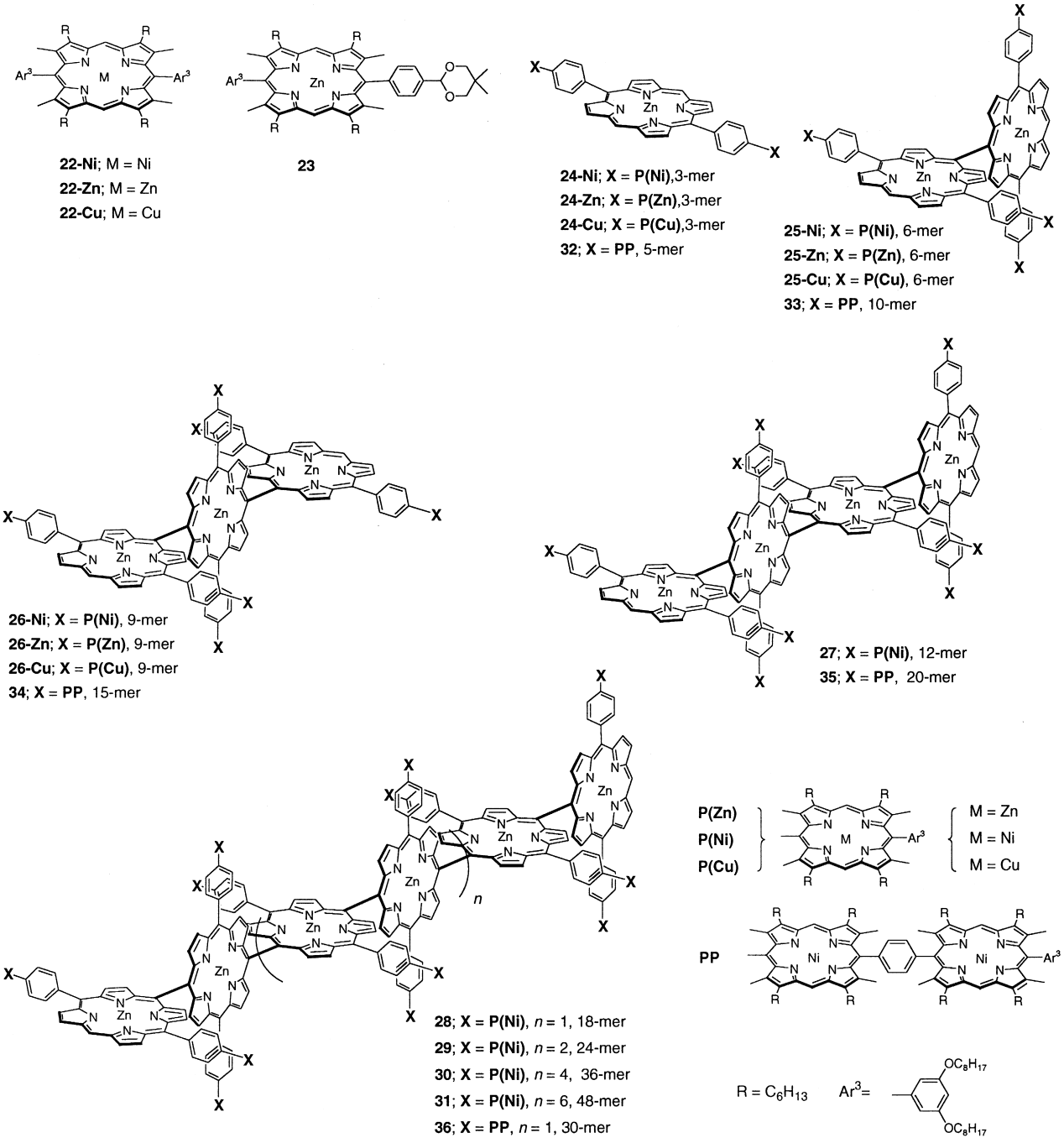

product was assigned as grid porphyrin 20-mer **35** (calcd for $C_{1120}H_{1450}N_{80}Ni_{16}O_{16}Zn_4$: 17491). We also isolated a larger molecule that eluted at 16.9 min (Figure 4e, right); this was tentatively assigned as grid porphyrin 30-mer **36**, although its molecular weight could not be determined. Further the grid porphyrin 12-mer **27** was coupled with 2.8 equivalents of $AgPF_6$ under the similar conditions to give higher oligomers (Figure 4c, left). Formation of distinct large molecules eluting at 17.3, 16.5, and 15.9 min, assignable to 24-mer, 36-mer, and 48-mer, respectively, was evident. The coupling reaction was stopped after 16 h, and all these products were separated in a pure form by recycling preparative GPC/HPLC. The molecular weights were determined by MALDI-TOF MS to be *m*/*z* 21466, 32276, and 43321, all in line with the expected grid porphyrin 24-mer **29**, 36-mer **30** (calcd for $C_{2064}H_{2666}N_{144}Ni_{24}O_{48}Zn_{12}$: 32456), and 48-mer **31** (calcd for $C_{2752}H_{3554}N_{192}Ni_{32}O_{64}Zn_{16}$: 43274), respectively. The structure of the porphyrin 48-mer **31**, the largest grid array prepared in this paper, is shown below. As described above, the MALDI-TOF MS measurement has been particularly effective in detecting molecular weights of these large porphyrin arrays (Table 2). ^1H NMR spectra should provide stronger evidence for their structure, including the coupling regiochemistry, but in most cases these large porphyrin arrays have rather broadened spectra with exceptions of the nonamer **26** and the 12-mer **27** (see, Experimental Section).

0947-6539/00/0617-3260 $ 17.50+.50/0 *Chem. Eur. J.* **2000**, *6*, No. 17

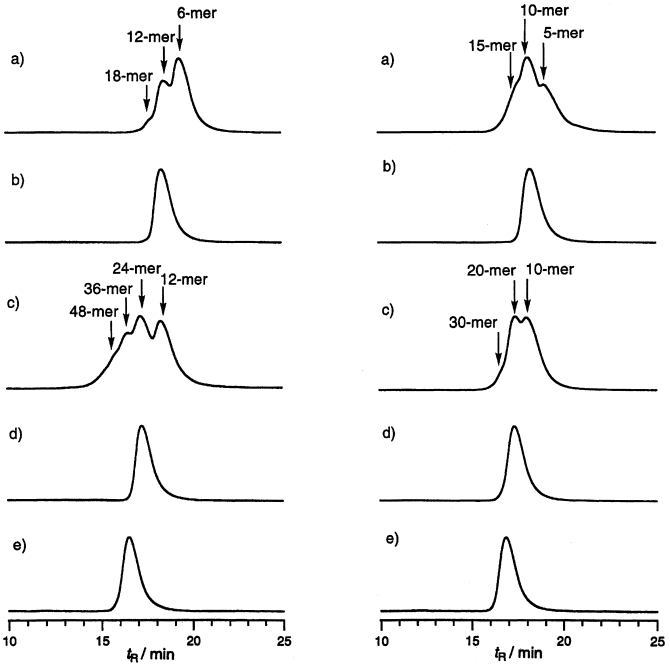

Figure 4. GPC/HPLC chromatograms of the Ag^I-promoted coupling reaction detected at 420 nm. Each chromatogram is normalized to the maximum intensity. Left: trimer series: a) the reaction of **25-Ni** with 2 equivalents of $AgPF_6$ for 9 h, b) purified 12-mer **27**, c) the reaction of **27** with 2.8 equivalents of $AgPF_6$ for 16 h, d) purified 24-mer **29**, and e) purified 36-mer **30**. Right: pentamer series: a) the reaction of **32** with 3.0 equivalents of $AgPF_6$ for 6 h, b) purified 10-mer **33**, c) the reaction of **33** with 3.1 equivalents of $AgPF_6$ for 16 h, d) purified 20-mer **35**, and e) purified 30-mer **36**.

The preparative GPC/HPLC is an essential technique for separation of these large porphyrin arrays and has been usually performed in a recycling manner, allowing the isolation of each porphyrin array in a pure state as indicated by a single peak (for example, Figure 4b, 4d and 4e, left and right). The relationship of the molecular weights of these porphyrin arrays versus the retention time in our GPC/HPLC set-up are summarized in Table 2 and Figure 5. Although these data contain the retention times of porphyrin arrays with different substituents and different molecular shape, inspection of these data has revealed that the retention time is roughly dependent upon the molecular weight of the porphyrin arrays; this results in a good linear relationship. However, the retention time also depends on the molecular shape, and the linear heptamer **16-Ni** and the windmill 14-mer **21-Ni** with longer wings elute slightly faster than the retention time expected on the basis of the above linear relationship, suggesting their larger hydrodynamic volume.

In addition to the elution behavior in the GPC/HPLC and the MALDI-TOF MS spectra, the UV-visible absorption spectra provided strong support for the homogeneity of the porphyrin arrays isolated. The absorption spectra of these porphyrin arrays and references are given in Figure 6 and Table 3. *meso*–*meso*-Linked linear porphyrin arrays, **2b** (dimer), **3b** (trimer), **4b** (tetramer), **5b** (hexamer), and **6b** (octamer) were synthesized and fully characterized.[17f] The absorption spectra of these arrays exhibit characteristic split Soret bands (Table 3), of which the Soret band of the higher energy portion is observed nearly at the same wavelength (ca.

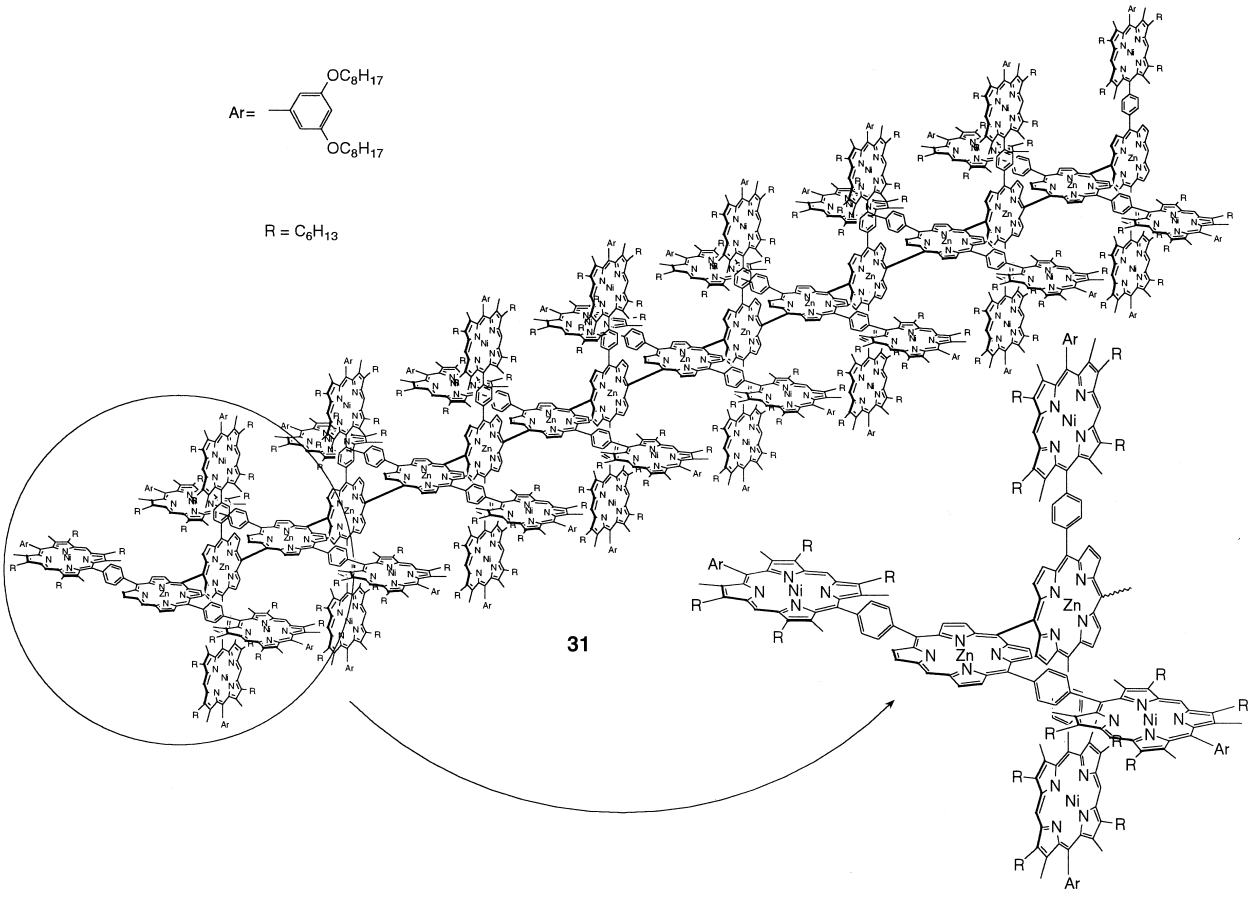

Table 2. Data of porphyrin arrays synthesized.

Compound[a]	shape[b]	molecular formula	calculated molecular weight	observed molecular weight[c]	retention time [min][d]
14-Ni (3)	L	$C_{158}H_{180}N_{12}Ni_2O_4Zn$	2493	2494	21.0
17-Ni (6)	W	$C_{316}H_{358}N_{24}Ni_4O_8Zn_2$	4985	4985	19.9
18 (9)	G	$C_{474}H_{536}N_{36}Ni_6O_{12}Zn_3$	7478	7476	19.3
15-Ni (5)	L	$C_{266}H_{320}N_{20}Ni_4O_4Zn$	4161	4160	20.1
19-Ni (10)	W	$C_{532}H_{638}N_{40}Ni_8O_8Zn_2$	8320	8321	18.9
20 (15)	G	$C_{798}H_{956}N_{60}Ni_{12}O_{12}Zn_3$	12481	–[e]	18.1
16-Ni (7)	L	$C_{374}H_{460}N_{28}Ni_6O_4Zn$	5829	5829	18.7
21-Ni (14)	W	$C_{748}H_{918}N_{56}Ni_{12}O_8Zn_2$	11656	11640	17.6
24-Ni (3)	L	$C_{172}H_{224}N_{12}Ni_2O_4Zn$	2706	2707	20.4
25-Ni (6)	W	$C_{344}H_{446}N_{24}Ni_4O_8Zn_2$	5411	5400	19.3
26-Ni (9)	G	$C_{516}H_{668}N_{36}Ni_6O_{12}Zn_3$	8115	8131	18.8
27 (12)	G	$C_{688}H_{890}N_{48}Ni_8O_{16}Zn_4$	10820	10822	18.4
28 (18)	G	$C_{1032}H_{1334}N_{72}Ni_{12}O_{24}Zn_6$	16229	16211	17.8
29 (24)	G	$C_{1376}H_{1778}N_{96}Ni_{16}O_{32}Zn_8$	21638	21466	17.3
30 (36)	G	$C_{2064}H_{2666}N_{144}Ni_{24}O_{48}Zn_{12}$	32456	32276	16.5
31 (48)	G	$C_{2752}H_{3554}N_{192}Ni_{32}O_{64}Zn_{16}$	43274	43321	15.9
32 (5)	L	$C_{280}H_{364}N_{20}Ni_4O_4Zn$	4374	4365	19.3
33 (10)	W	$C_{560}H_{726}N_{40}Ni_8O_8Zn_2$	8746	8741	18.3
34 (15)	G	$C_{840}H_{1088}N_{60}Ni_{12}O_{12}Zn_3$	13119	13038	17.8
35 (20)	G	$C_{1120}H_{1450}N_{80}Ni_{16}O_{16}Zn_4$	17491	17426	17.4
36 (30)	G	$C_{1680}H_{2174}N_{120}Ni_{24}O_{24}Zn_6$	26236	–[e]	16.9

[a] Number in the parentheses indicates the number of the porphyrins in the array. [b] L = linear, W = windmill, G = grid. [c] Determined by MALDI-TOF MS. [d] Retention time on analytical GPC/HPLC. For details, see Experimental Section. [e] Not detected.

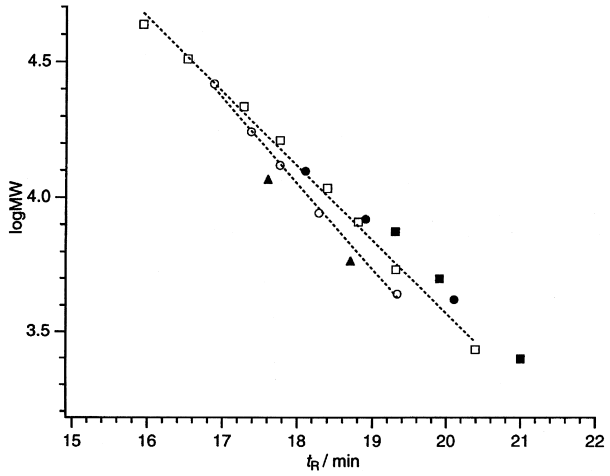

Figure 5. Relationship of the retention time versus log MW. Filled square: **14-Ni**, **17-Ni**, **18**; filled circle: **15-Ni**, **19-Ni**, **20**; filled triangle: **16-Ni**, **21-Ni**; open square: **24 – 31**; open circle: **32 – 36**.

414 nm), while the Soret band of the lower energy portion undergoes a systematic red-shift with increasing number of porphyrins (450 nm in **2b** to 500 nm in **6b**). Such red-shifted split Soret bands were clearly visible in the absorption spectra of the windmill and grid porphyrin arrays (Figure 6, designated by arrows in each spectrum) at the same wavelength as those of the reference *meso – meso*-linked porphyrin arrays **2b – 6b** (Table 3).

Mechanistic studies on formation of windmill hexamers: As described above, the Ag^I-promoted coupling reaction of 1,4-phenylene-bridged linear porphyrin arrays proceeded efficiently, giving the corresponding windmill porphyrin arrays with good yields and excellent *meso – meso* regioselectivity. It is interesting to note that the coupling reactions of 1,4-phenylene-bridged porphyrin trimers proceeded at similar rate to or even faster than that of the parent porphyrin monomer. Therefore it may be suggested that the peripheral Ni^{II} β-octaalkylporphyrins act as a mediator for the oxidation of the central Zn^{II} β-free porphyrin by the Ag^I ion. This mechanism is supported by the fact that the first one-electron oxidation of Zn^{II} β-free porphyrin (0.30 V) is similar to that of Ni^{II} β-octaalkylporphyrin (0.32 V) and that the Ni^{II} β-octaalkylporphyrins spatially surround the Zn^{II} β-free porphyrin and thus are more accessible to the Ag^I ion. Namely, the initial oxidation of the peripheral Ni^{II} porphyrin by an Ag^I ion followed by a hole transfer to the central Zn^{II} β-free porphyrin may assist generation of the radical cation of the central Zn^{II} β-free porphyrin. In order to examine this possibility, we prepared three linear trimers **24-Zn**, **24-Ni**, and **24-Cu** and compared the relative rates of the *meso – meso*-coupling reactions.

The coupling reactions of **24-Zn**, **24-Ni**, and **24-Cu** were performed with two equivalents of $AgPF_6$ at room temperature in $CHCl_3$ for 5 – 10 h to give the corresponding windmill porphyrin hexamers **25-Zn**, **25-Ni**, and **25-Cu** and corresponding trimeric nonamers. After usual workup and separation by preparative GPC/HPLC, the windmill hexamers **25-Zn**, **25-Ni**, and **25-Cu** were obtained in 30 – 48 % yields. Progress of the reactions of **24-Zn**, **24-Ni**, **24-Cu**, and **1a** was monitored by the analytical GPC/HPLC (Figure 7). The coupling reactions of the trimers, **24-Zn**, **24-Ni**, and **24-Cu**, were faster than that of the parent **1a** (Figure 7, at the reaction time of 6 h). The initial reaction of **24-Zn** was distinctly faster than **24-Ni** and **24-Cu**; this suggests a superior coupling – accelerating role of the peripheral Zn^{II} β-octaalkylporphyrins over those of the corresponding Ni^{II} and Cu^{II} β-octaalkylporphyrins. Since it was rather difficult to determine the one electron oxidation potentials of each subunit in the porphyrin trimers **24-Zn**, **24-Ni**, and **24-Cu**, we used the oxidation potentials of the reference monomers (**22-Zn**, 0.16 V; **22-Ni**, 0.27 V; **22-Cu**, 0.30 V, in $CHCl_3$ vs. a ferrocene/ferrocenium ion couple) in the following discussion. A plausible mechanism is outlined in Scheme 5 in which trimer was indicated as Z2-Z1-Z2, where Z1 and Z2 represent a Zn^{II} β-free porphyrin and a metallated β-octaalkylporphyrin, respectively. We would like to propose here, in addition to direct oxidation of Z1 by an Ag^I ion, the presence of indirect oxidation pathway through the initial oxidation of Z2 with an Ag^I ion followed by hole transfer from Z2 to Z1 for the generation of $Z1^+$. Indirect routes have

0947-6539/00/0617-3262 $ 17.50+.50/0 *Chem. Eur. J.* **2000**, *6*, No. 17

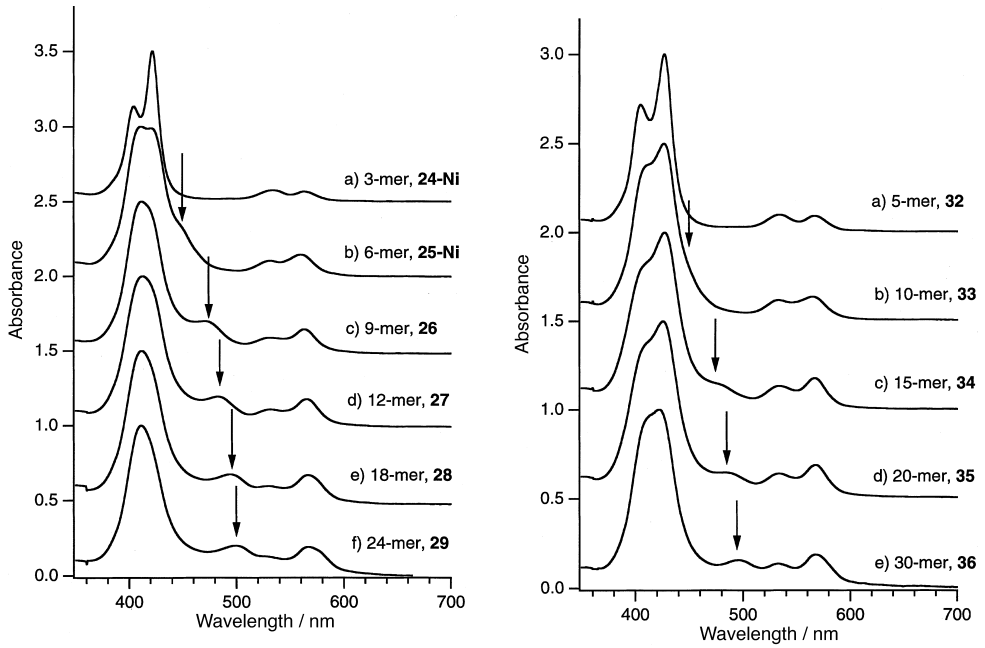

Figure 6. Absorption spectra in CH_2Cl_2. Left: trimer series. Right: pentamer series. Absorbances are normalized at the maximum intensity. Arrows indicate the red-shifted Soret band of the *meso*–*meso*-linked porphyrin oligomers.

Table 3. Absorption spectra of grid porphyrin arrays and *meso*–*meso*-linked porphyrin arrays.

Number of the unit [a]	Compound[b]	Absorption data[c,d] [nm]	Compound[b]	Absorption data[d] [nm]	Compound[b]	Absorption data[d] [nm]
1	**1b** (1)	413, 538	**24-Ni** (3)	405, 422, 535, 563	**32** (5)	405, 427, 534, 567
2	**2b** (2)	417, 450, 556	**25-Ni** (6)	411, 421, 451 (sh), 532, 560	**33** (10)	408 (sh), 427, 533, 566[e]
3	**3b** (3)	414, 474, 566	**26-Ni** (9)	412, 471, 533, 563	**34** (15)	405 (sh), 428, 480 (sh), 534, 567
4	**4b** (4)	414, 486, 573	**27** (12)	413, 483, 532, 566	**35** (20)	407 (sh), 426, 484, 534, 568
6	**5b** (6)	414, 495, 579	**28** (18)	412, 494, 531, 567	**36** (30)	422, 496, 533, 568
8	**6b** (8)	414, 500, 582	**29** (24)	412, 500, 567		

[a] Number of the *meso*–*meso*-linked porphyrin cores in each array. [b] Number in the parentheses indicates the number of the porphyrins in the array. [c] Ref. [17f]. [d] Peaks of the red-shifted Soret band of *meso*–*meso*-linked porphyrin cores are underlined. [e] The red-shifted Soret band is hidden.

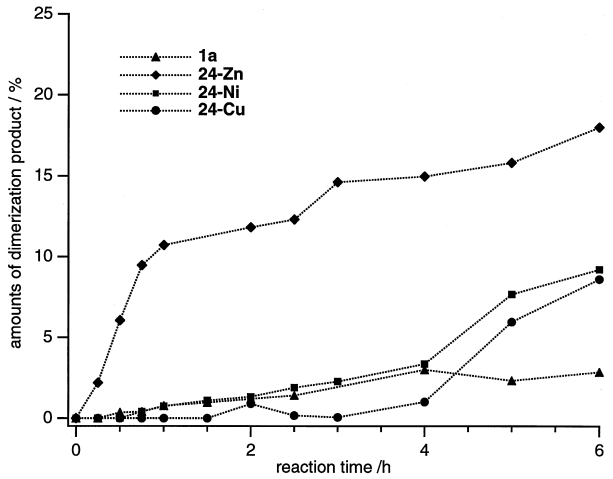

Figure 7. Progress of the reactions of **1a**, **24-Zn**, **24-Ni**, and **24-Cu**. Product distribution was determined from GPC/HPLC analysis.

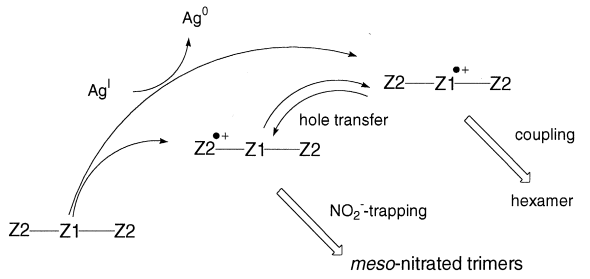

Scheme 5. Proposed mechanism of the Ag^I-promoted oxidative coupling reaction of porphyrin trimer Z2-Z1-Z2.

several advantages; the initial oxidation reaction of Z2 is less endothermic compared with the direct oxidation of Z1 and it is entropically favorable, since the available oxidation sites are twofold. In addition, the second hole transfer from Z2 to Z1 is an intramolecular process and is also entropically favored. The initial oxidation step must be most favorable in **24-Zn**, since it has the least activation energy. It is also notable that the material balance of the reaction of **24-Zn** was excellent without serious side reactions in contrast to the reaction of **10-Zn**; this suggests that a minor structural change at the peripheral Zn^{II} β-octaalkylporphyrin subunit can lead to suppression of the undesirable side reactions of its radical cation under these conditions.

In order to gain a further support for this mechanism, we attempted to trap the radical cation intermediate of the peripheral porphyrins by using a small electrophile that is known to react with the radical cation of Zn^{II} β-octaalkylporphyrin. We chose the reaction with $AgNO_2$, since it has been demonstrated that radical cation of Zn^{II} β-octaalkylporphyrin can be trapped by $AgNO_2$ to give a *meso*-nitrated porphyrin through nucleophilic attack by NO_2^-.[25] However, reaction of **24-Zn** with $AgNO_2$ did not give any nitration products. After several unsuccessful trapping trials, we thought that the nucleophilic trapping might be hampered owing to steric hindrance of the flanking bulky β-hexyl groups. We thus examined the reaction of trimeric porphyrin **37**, which bears small β-ethyl substituents instead of β-hexyl substituents. Under the normal coupling conditions (2.1 equiv $AgPF_6$, $CHCl_3$, room temperature, 4 h), the trimer **37** was converted into the corresponding hexamer **38**. We then examined the reaction of **37** with 2.1 equivalents of $AgNO_2$. After 6 h, the MALDI-TOF MS analysis of the reaction mixture indicated the formation of trimers with molecular weights of *m*/*z* 2318 and 2362, as well as a peak at *m*/*z* 2271 due to the starting trimer **37**. These new molecular peaks are consistent with mononitrated porphyrin **39** (calcd for $C_{140}H_{159}N_{13}O_6Zn_3$: 2316) and dinitrated porphyrin **40** (calcd for $C_{140}H_{158}N_{14}O_8Zn_3$: 2361). Interestingly, the formation of the windmill porphyrin array **38** was not detected at all in this reaction. These products were separated by silica gel chromatography to **37**, **39**, and **40** in 16%, 30%, and 21% yields, respectively. The ^{1}H NMR spectrum of **39** showed three signals for the *meso* protons in a ratio of 2:2:1 at $\delta = 10.56$ (H^a), 10.35 (H^b), and 10.14 (H^c) and six signals for the β-methyl group protons in a ratio of 6:3:3:6:3:3, indicating the nitration at the *meso*-position of the peripheral porphyrin. The ^{1}H NMR spectrum of **40** indicated two different *meso* protons in a ratio of 1:1 at $\delta = 10.57$ (H^a) and 10.14 (H^c), and four different β-methyl group protons ($6H \times 4$), revealing that the each peripheral porphyrin is mononitrated at the *meso*-position. In summary, the Ag^I-promoted oxidation reaction of **37** gives the *meso*–*meso*-coupled hexamer **38** in the absence of a small nucleophile, but leads to formation of the nitration products **39** and **40** in the present of NO_2^-. The results are consistent with the proposed mechanism in Scheme 5. Probably, the reaction of **37** with $AgPF_6$ begins with oxidation of the more electron-rich peripheral Zn^{II} β-octaalkylporphyrins, and the resulting radical cation of Zn^{II} β-free porphyrin is effectively trapped by NO_2^- before the endothermic intramolecular hole transfer. The absence of **38** in the reaction of **37** with $AgNO_2$ indicated that the trapping by NO_2^- is faster than the hole transfer. This hole-hopping behavior, which involves the peripheral porphyrins as a mediator, is interesting in that the coupling reaction is significantly accelerated but does not lose the high regio-selectivity.

Intramolecular singlet excitation energy transfer in all zinc(II) windmill porphyrin arrays: Structurally well-defined architectures of these windmill and grid porphyrin arrays may be attractive for use in a variety of fields such as nanoscale optical and electrochemical molecular devices. Here we report intramolecular energy transfer in the all Zn^{II}-metallated windmill porphyrin arrays **11-Zn**, **14-Zn**, and **15-Zn**.

In order to examine the photochemical properties of the windmill porphyrin arrays, the arrays containing Ni^{II} (**10-Ni**, **11-Ni**, **14-Ni**, **15-Ni**, **17-Ni**, and **19-Ni**) were all transformed into the corresponding all Zn^{II}-metallated porphyrin arrays, **10-Zn**, **11-Zn**, **14-Zn**, **15-Zn**, **17-Zn**, and **19-Zn** by demetallation with TFA and 10% H_2SO_4 in refluxing toluene followed by Zn^{II} ion insertion with $Zn(OAc)_2$. The absorption and fluorescence spectra of **2a** and **23** as component of the windmill porphyrin arrays are shown in Figure 8. The peripheral porphyrin **23** has a sharp Soret band at 410 nm

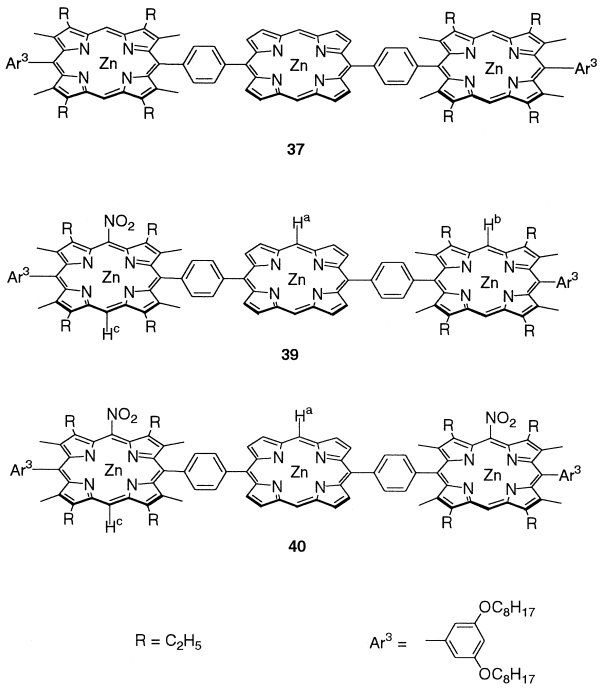

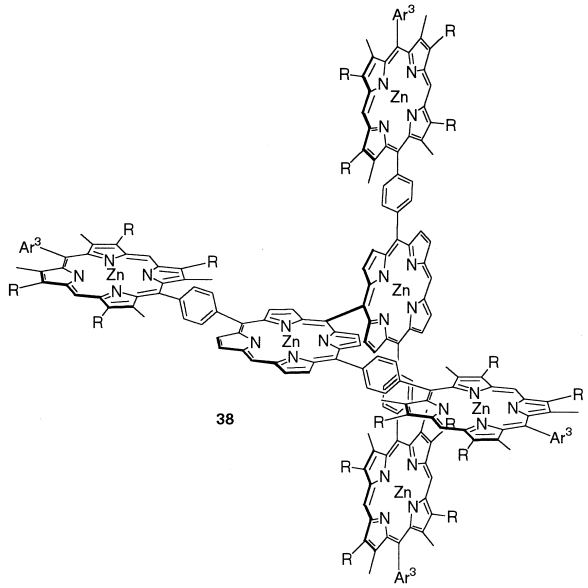

0947-6539/00/0617-3264 $ 17.50+.50/0 *Chem. Eur. J.* **2000**, *6*, No. 17

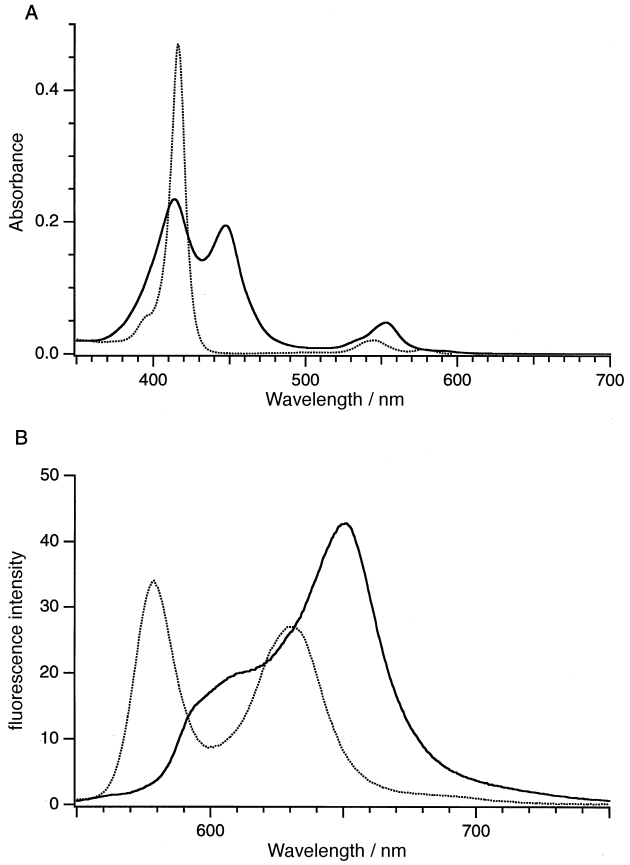

Figure 8. A) Absorption and B) fluorescence spectra of **2a** (solid lines) and **23** (dotted lines). Fluorescence spectra were taken for excitation at 540 nm at which the absorbance was adjusted at 0.05.

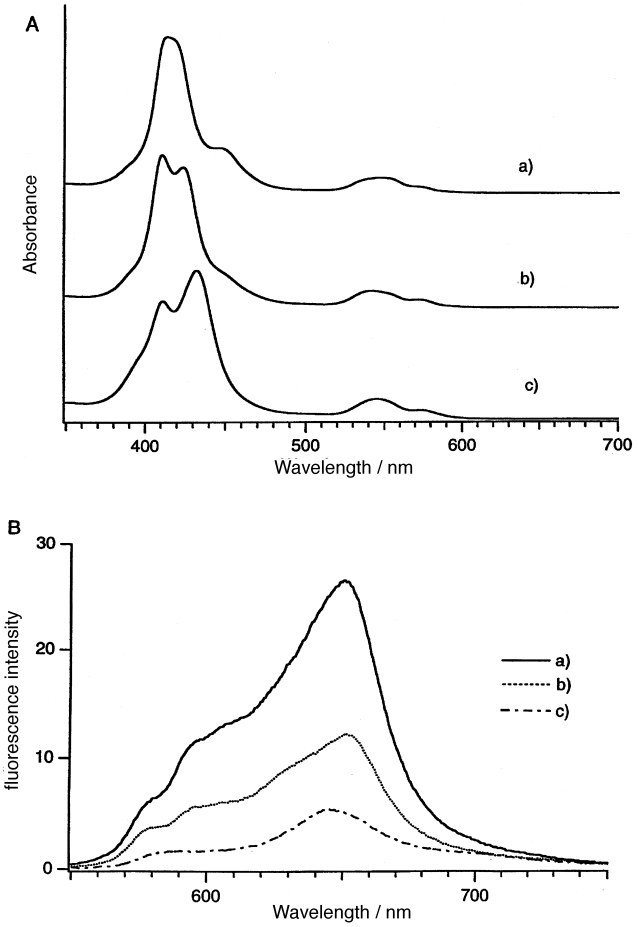

Figure 9. A) Absorption and B) fluorescence spectra of windmill porphyrin arrays in CH_2Cl_2: a) **11-Zn**, b) **17-Zn**, and c) **19-Zn**. Absorbances are normalized at the maximum intensity, and fluorescence spectra were taken for excitation at 540 nm at which the absorbance was adjusted at 0.05.

and Q-bands at 538 and 574 nm and exhibits the fluorescence emission with two bands at 579 and 632 nm, while **2a** displays split Soret bands at 414 and 447 nm and broader and red-shifted fluorescence at 651 nm. The fluorescence quantum yields of **2a** and **23**, determined relative to the reported value (0.03 for Zn^{II} TPP in benzene),[26] are 0.033 and 0.024, respectively. The absorption spectrum of the windmill porphyrin tetramer **11-Zn** shows a broad Soret band at 414 nm and a shoulder at 447 nm (Figure 9A, curve a). A broad or split Soret band is characteristic for a 1,4-phenylene-bridged Zn^{II}-diporphyrin unit as reported previously.[21, 27] The shoulder can be assigned as a low-energy portion of split Soret bands as observed in the *meso*–*meso*-linked porphyrin dimer **2a**.[17] As with **11-Zn**, the absorption spectrum of the hexamer **17-Zn** exhibits a shoulder at about 450 nm due to the lower energy portion of split Soret bands, but such a band is almost hidden in the absorption spectrum of **19-Zn**. The steady-state fluorescence spectra of **11-Zn**, **17-Zn** and **19-Zn** are all quite similar in shape to that of **2a**, indicating that most of the emission is coming from the *meso*–*meso*-linked diporphyrin core. The fluorescence quantum yields of the arrays are 0.023, 0.012, and 0.0050, respectively. Closer examination revealed that the fluorescence is composed of dual emissions from the peripheral porphyrins ($\lambda_{max} = 579$ and 632 nm) and from the *meso*–*meso*-linked diporphyrin core ($\lambda_{max} = 651$ nm) (Figure 9B). The fluorescence intensity of the peripheral porphyrins is reduced and that of the *meso*–*meso*-linked diporphyrin core is enhanced; this indicates the singlet–singlet energy transfer from the peripheral porphyrins to the diporphyrin core. This energy transfer can be rationalized in terms of the lower energy level of the S_1 state of the diporphyrin subunit (2.07 eV) relative to that of the Zn^{II} peripheral porphyrin (2.13 eV). The time-resolved picosecond fluorescence spectra[28] of **11-Zn** (not shown)[19] and **17-Zn** (Figure 10) provided more support for the energy transfer, since the emission from the S_1 state of the peripheral porphyrins that predominated at an early stage decayed rapidly, and the broad emission from the S_1 state of the *meso*–*meso*-linked diporphyrin core increased gradually following the energy transfer.

The fluorescence decay at 585 nm of **11-Zn**, which was due mainly to the emission from the energy donor peripheral porphyrins, can be fit with a biexponential function with time constants of 34 ps (64%) and 1.56 ns (36%), and that of **17-Zn** can be fit with a biexponential function with time constants of 56 ps (73%) and 1.62 ns (27%). The observed biphasic fluorescence decay behaviors and a small energy difference (0.06 eV) between the donor and the acceptor led us to suggest the reaction shown in Scheme 6, in which a rapid equilibrium between the excited states, $^1P^*$-C and P-$^1C^*$ is achieved. Here P and C represent a peripheral porphyrin monomer and a central *meso*–*meso*-linked diporphyrin core

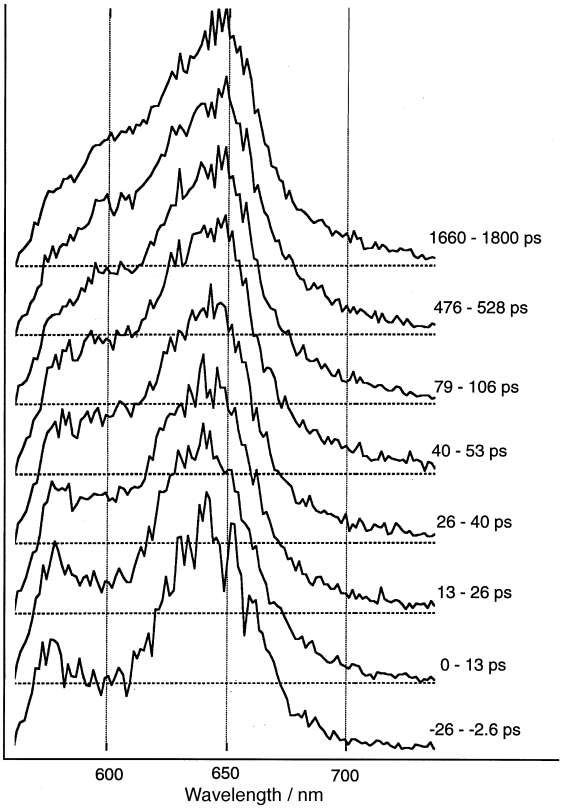

Figure 10. Time-resolved fluorescence spectra of **17-Zn** in CH_2Cl_2 at room temperature for the excitation at 532 nm.

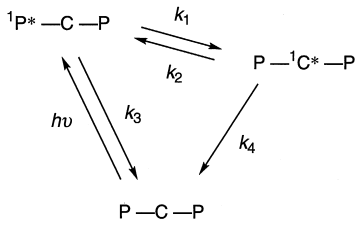

Scheme 6. Energy transfer of windmill porphyrin arrays.

in the windmill porphyrin arrays, respectively. Such an equilibrium may be plausible, since the energy levels of the two excited states are close to each other. According to this scheme, the fluorescence decay behavior of ^{1}P* can be expressed by Equation (1).

$$[1P^* - C] = C_1 e^{-\alpha t} + C_2 e^{-\beta t} \quad (1)$$

$$\alpha = \tfrac{1}{2}\left[(k_1 + nk_2 + k_3 + k_4) + \sqrt{(k_1 - nk_2 + k_3 - k_4)^2 + 4k_1k_2}\right] \quad (2)$$

$$\beta = \tfrac{1}{2}\left[(k_1 + nk_2 + k_3 + k_4) - \sqrt{(k_1 - nk_2 + k_3 - k_4)^2 + 4k_1k_2}\right] \quad (3)$$

The rate constants of the intramolecular energy transfer, k_1 and k_2, were calculated by the well-established procedure [Eqs. (2) and (3)], in which k_1, k_2, k_3, and k_4 are defined in Scheme 6, n is the number of the donor porphyrins in the array (two for the tetramer **11-Zn**, four for the hexamer **17-Zn**), and α and β are the experimental values that, ideally, can be determined from the fluorescence decay analysis. With values of $k_3 = 8.2 \times 10^8\ s^{-1}$ and $k_4 = 5.9 \times 10^8\ s^{-1}$, k_1 and k_2 were calculated; $k_1 = 2.8 \times 10^{10}\ s^{-1}$, $k_2 = 4.8 \times 10^7\ s^{-1}$ for **11-Zn** and $k_1 = 1.7 \times 10^{10}\ s^{-1}$, $k_2 = 8.3 \times 10^8\ s^{-1}$ for **17-Zn**. Therefore, it turns out that the effects of back energy transfer are very actually small. Time-resolved fluorescence spectra of **19-Zn** (not shown) are also similar to those of **11-Zn**; this indicates the efficient excitation energy transfer from the peripheral porphyrins to the diporphyrin core similarly even in larger porphyrin arrays. The fluorescence decay at 585 nm of **19-Zn** was also analyzed as a biexponential function with lifetimes of 85 ps (90%) and 1.28 ns (10%). However, the photoexcited dynamics of **19-Zn** must be more complicated because of the degenerate and seemingly reversible energy hopping between the same two peripheral porphyrins; therefore, further analysis has not carried out. In summary, the windmill arrays **11-Zn**, **17-Zn**, and **19-Zn** have light-energy-funneling functions from the peripheral porphyrins to the diporphyrin core, but the efficiency is not quantitative mostly owing to an insufficient energy gap between the energy donor and acceptor.

Conclusion

The Ag^I-promoted block oligomerization of the 1,4-phenylene-bridged linear porphyrin arrays and the windmill porphyrin arrays led to an efficient construction of three-dimensionally arranged windmill and grid porphyrin arrays. The coupling proceeded regioselectively only at the *meso*-position of Zn^{II} β-free porphyrin. These multiporphyrin arrays are characterized by 1) good solubility in various organic solvents in spite of large molecular size and extended aggregation tendency of multiporphyrin arrays, 2) easy extension to higher arrays with well-defined geometries, 3) easy separation over the recycling preparative GPC/HPLC, 4) controlled interporphyrin distances and angles and thus controlled interporphyrin electronic interactions, and 5) the efficient singlet energy transfer from the peripheral porphyrins to the central diporphyrin core in the all Zn^{II}-metallated complexes. Further elaboration of these arrays toward photosynthetic functions is an attractive future target and is actively pursued in our laboratory.

Experimental Section

General: All reagents and solvents were of the commercial reagent grade and were used without further purification except where noted. Dry CH_2Cl_2, $CHCl_3$, and acetonitrile were obtained by heating under reflux and distillation over CaH_2. Solvents used for spectroscopic measurements were all spectroscopic grade. Preparative separations were performed by silica-gel gravity-flow column chromatography (Wako wakogel C-200), silica-gel flash column chromatography (Merck Kieselgel 60H Art. 7736), and gel-permeation chromatography (GPC; Bio-Rad Bio-Beads S-X1, packed with toluene). Separations of the large porphyrin arrays were performed by recycling preparative HPLC (Japan Analytical Industry, LC-908 with JAIGEL 2.5H, 3H, and 4H columns in series) with $CHCl_3$ as an eluent. Analytical HPLC was performed on JAIGEL-2.5H-AF, 3H-AF, and 4H-AF columns in series (eluent, $CHCl_3$; flow rate, 1.2 mL min^{-1}; detected at 400–700 nm) with a JASCO HPLC apparatus with a multi-wavelength detector MD-915. Product distributions were determined on the basis of the HPLC chart after appropriate calibration. ^{1}H NMR spectra were recorded in a $CDCl_3$ solution on a JEOL ALPHA-500 spectrometer (operating at 500 MHz), and chemical shifts were represented as δ values in

0947-6539/00/0617-3266 $ 17.50+.50/0 *Chem. Eur. J.* **2000**, *6*, No. 17

ppm relative to the internal standard of $CHCl_3$ ($\delta = 7.260$). FAB mass spectra were recorded on a JEOL HX-110 spectrometer with the positive-FAB ionization method (accelerating voltage: 10 kV; primary ion sources: Xe) and 3-nitrobenzylalcohol matrix, and MALDI-TOF mass spectra were recorded on a KRATOS PC-KOMPACT SHIMADZU MALDI 4 spectrometer using positive-MALDI-TOF method with/without sinapinic acid matrix. UV/Vis absorption spectra were recorded on a Shimadzu UV-2400PC spectrometer. Steady-state fluorescence emission spectra were recorded on a Shimadzu RF-5300PC spectrofluorometer. Redox potentials were measured by the cyclic voltammetry method and differential pulse voltammetry method on a ALS electrochemical analyzer model 660. Fluorescence decay curves and time-resolved fluorescence spectra were measured by using a picosecond time-correlated single-photon-counting apparatus.[28]

General procedure for porphyrin metallation: For the metallation with Zn^{II}, a saturated solution of $Zn(OAc)_2$ in MeOH was adde to a solution of free base porphyrin in CH_2Cl_2, and the resulting mixture was stirred for 1–2 h. After the complete metallation was confirmed by TLC and UV analyses, the mixture was poured into water, and the porphyrin products were extracted with CH_2Cl_2. The organic layer was separated and the combined extracts were washed with water and brine, and dried over anhydrous Na_2SO_4. Further purification was carried out by silica gel column chromatography to give the Zn^{II} porphyrin. For the metallation with Ni^{II}, we used toluene as a solvent and $Ni(acac)_2$ as a metal salt. The metallation was performed by heating the reaction mixture under reflux for 5–6 h in the dark. For the metallation with Cu^{II}, we used CH_2Cl_2 as a solvent and a saturated solution of $Cu(OAc)_2$ in MeOH as a metallating reagent. The metallation was performed by heating the reaction mixture under reflux for 1–2 h in the dark.

1,4-Phenylene-bridged Zn^{II}-Ni^{II} porphyrin dimer 10-Ni: Formyl-substituted porphyrin **7-Ni** (84.5 mg, 0.0775 mmol), 3,5-di-*tert*-butylbenzaldehyde **9** (34 mg, 0.158 mmol), and 2,2′-dipyrrylmethane **8** (34 mg, 0.234 mmol) were dissolved in dry CH_2Cl_2 (30 mL). After addition of trifluoroacetic acid (0.050 mL), the solution was stirred for 11 h at room temperature under N_2 in the dark. Then *p*-chloranil (0.273 mmol) was added to the solution, and the mixture was stirred for an additional 5.5 h. After addition of triethylamine (0.5 mL), the reaction mixture was poured into water, and the porphyrin products were extracted with CH_2Cl_2. The combined organic extract was successively washed with water, HCl (1N), aqueous $NaHCO_3$, and brine, and dried over anhydrous Na_2SO_4. After the zinc metallation, separation over silica gel column chromatography (eluent: CH_2Cl_2) gave the desired diporphyrin **10-Ni** (30.5 mg, 0.0188 mmol, 12%). ^{1}H NMR: $\delta =$ 10.40 (s, 2H; *meso*), 9.57 (m, 4H; *meso*, *β*-H), 9.51 (d, 2H; *β*-H), 9.45 (d, 2H; *β*-H), 9.27 (d, 2H; *β*-H), 8.52 (d, $J = 8.0$ Hz, 2H; Ar), 8.32 (d, $J =$ 8.0 Hz, 2H; Ar), 8.21 (d, $J = 2.0$ Hz, 2H; Ar), 7.90 (s, 1H; Ar), 7.81 (d, $J =$ 7.5 Hz, 2H; Ar), 7.48 (d, $J = 7.5$ Hz, 2H; Ar), 6.89 (d, $J = 8.5$ Hz, 1H; Ar), 6.87 (d, $J = 3.0$ Hz, 1H; Ar), 6.81 (dd, $J = 8.5$, 3.0 Hz, 1H; Ar), 4.24 (s, 2H; Ar-CH_2-Ar), 3.86 (s, 3H; OMe), 3.82 (s, 3H; OMe), 3.86 (t, $J = 7.5$ Hz, 4H; hexyl), 3.72 (t, $J = 7.5$ Hz, 4H; hexyl), 2.94 (s, 6H; Me), 2.33 (s, 6H; Me), 2.20 (m, 4H; hexyl), 2.07 (m, 4H; hexyl), 1.42 (s, 18H; *t*Bu), 1.79–1.39 (m, 24H; hexyl), 0.99–0.93 (m, 12H; hexyl); MS (FAB): found 1621; calcd for $C_{103}H_{116}N_8NiO_2Zn$: 1621; UV/Vis (benzene): $\lambda_{max} = 420.5$ (Soret), 537.0, 564.5 nm.

1,4-Phenylene-bridged Ni^{II}-Zn^{II}-Ni^{II} porphyrin trimer 14-Ni: Formyl-substituted porphyrin **7-Ni** (204 mg, 0.187 mmol), and 2,2′-dipyrrylmethane **8** (34 mg, 0.234 mmol) were dissolved in dry CH_2Cl_2 (40 mL). After addition of trifluoroacetic acid (0.040 mL), the solution was stirred for 2 h at room temperature under N_2 in the dark. Then *p*-chloranil (0.285 mmol) was added to the solution, and the mixture was stirred for an additional 1 h. After addition of triethylamine, the reaction mixture was poured into water, and the porphyrin products were extracted with CH_2Cl_2. The combined organic extract was successively washed with water, HCl solution (1N), aqueous $NaHCO_3$, and brine, and dried over anhydrous Na_2SO_4. After the zinc metallation, separation over silica gel column chromatography (eluent: CH_2Cl_2) gave the desired triporphyrin **14-Ni** (118.4 mg, 0.0475 mmol, 51%). ^{1}H NMR: $\delta = 10.55$ (s, 2H; *meso*), 9.68 (d, $J = 4.0$ Hz, 4H; *β*-H), 9.57 (s, 4H; *meso*), 9.53 (d, $J = 4.5$ Hz, 4H; *β*-H), 8.59 (d, $J =$ 8.0 Hz, 4H; Ar), 8.35 (d, $J = 8.0$ Hz, 4H; Ar), 7.80 (d, $J = 7.0$ Hz, 4H; Ar), 7.49 (d, $J = 7.0$ Hz, 4H; Ar), 6.92 (d, $J = 8.5$ Hz, 2H; Ar), 6.89 (d, $J = 4.0$ Hz, 2H; Ar), 6.84 (dd, $J = 8.5$, 3.5 Hz, 2H; Ar), 4.26 (s, 4H; Ar-CH_2-Ar), 3.90 (s, 6H; OMe), 3.84 (s, 6H; OMe), 3.86 (t, $J = 7.5$ Hz, 8H; hexyl), 3.72 (t, $J =$ 7.5 Hz, 8H; hexyl), 2.96 (s, 12H; Me), 2.32 (s, 12H; Me), 2.18 (m, 8H; hexyl), 2.08 (m, 8H; hexyl), 1.78 (m, 8H; hexyl), 1.68 (m, 8H; hexyl), 1.54–1.39 (m, 32H; hexyl), 0.99–0.94 (m, 24H; hexyl); MS (FAB): found 2494; calcd for $C_{158}H_{180}N_{12}Ni_2O_4Zn$: 2493; UV/Vis (benzene): $\lambda_{max} = 408.0$ (Soret), 424.5 (Soret), 534.0, 563.5 nm.

1,4-Phenylene-bridged Ni^{II}-Ni^{II}-Zn^{II}-Ni^{II}-Ni^{II} porphyrin pentamer 15-Ni: This porphyrin pentamer was prepared from formyl-substituted diporphyrin **12-Ni** (193.9 mg, 0.101 mmol) and **8** (21.7 mg, 0.148 mmol) by the procedure used for the preparation of **14-Ni**. Yield of **15-Ni** was 68% (141.8 mg, 0.0341 mmol). ^{1}H NMR: $\delta = 10.55$ (s, 2H; *meso*), 9.69 (d, $J =$ 4.5 Hz, 4H; *β*-H), 9.60 (s, 4H; *meso*), 9.55 (d, $J = 4.5$ Hz, 4H; *β*-H), 9.46 (s, 4H; *meso*), 8.61 (d, $J = 7.5$ Hz, 4H; Ar), 8.38 (d, $J = 7.5$ Hz, 4H; Ar), 8.20 (s, 8H; Ar), 7.77 (d, $J = 8.0$ Hz, 4H; Ar), 7.47 (d, $J = 8.0$ Hz, 4H; Ar), 6.92 (d, $J = 8.5$ Hz, 2H; Ar), 6.88 (d, $J = 3.0$ Hz, 2H; Ar), 6.83 (dd, $J = 8.5$, 3.0 Hz, 2H; Ar), 4.25 (s, 4H; Ar-CH_2-Ar), 3.89 (s, 6H; OMe), 3.83 (s, 6H; OMe), 3.89–3.67 (m, 32H; hexyl), 2.98 (s, 12H; Me), 2.84 (s, 12H; Me), 2.81 (s, 12H; Me), 2.36 (s, 12H; Me), 2.25–2.02 (m, 32H; hexyl), 1.83–1.26 (m, 96H; hexyl), 1.00–0.92 (m, 48H; hexyl); MS(TOF): found 4160; calcd for $C_{266}H_{320}N_{20}Ni_4O_4Zn$: 4161; UV/Vis (benzene): $\lambda_{max} = 409.5$ (Soret), 429.5 (Soret), 537.0, 567.5 nm.

1,4-Phenylene-bridged Ni^{II}-Ni^{II}-Ni^{II}-Zn^{II}-Ni^{II}-Ni^{II}-Ni^{II} porphyrin heptamer 16-Ni: This porphyrin heptamer was prepared from formyl-substituted triporphyrin **13-Ni** (48.2 mg, 0.0175 mmol) and **8** (8.1 mg, 0.056 mmol) by the procedure used for the preparation of **14-Ni**. Yield of **16-Ni** was 80% (41.2 mg, 0.0071 mmol). ^{1}H NMR: $\delta = 10.56$ (s, 2H; *meso*), 9.70 (d, $J =$ 4.0 Hz, 4H; *β*-H), 9.62 (s, 4H; *meso*), 9.55 (d, $J = 3.5$ Hz, 4H; *β*-H), 9.50 (s, 4H; *meso*), 9.46 (s, 4H; *meso*), 8.62 (d, $J = 7.5$ Hz, 4H; Ar), 8.38 (d, $J =$ 7.5 Hz, 4H; Ar), 8.23 (s, 8H; Ar), 8.18 (s, 8H; Ar), 7.77 (d, $J = 7.5$ Hz, 4H; Ar), 7.47 (d, $J = 7.5$ Hz, 4H; Ar), 6.92 (d, $J = 9.0$ Hz, 2H; Ar), 6.88 (d, $J =$ 3.0 Hz, 2H; Ar), 6.83 (dd, $J = 9.0$, 3.0 Hz, 2H; Ar), 4.25 (s, 4H; Ar-CH_2-Ar), 3.89 (s, 6H; OMe), 3.84 (s, 6H; OMe), 3.76–3.67 (m, 48H; hexyl), 2.98 (s, 12H; Me), 2.85 (s, 12H; Me), 2.83 (s, 12H; Me), 2.80 (s, 12H; Me), 2.79 (s, 12H; Me), 2.28 (s, 12H; Me), 2.10–2.02 (m, 48H; hexyl), 1.72–1.40 (m, 144H; hexyl), 1.03–0.92 (m, 72H; hexyl); MS (TOF): found 5829; calcd for $C_{374}H_{460}N_{28}Ni_6O_4Zn$: 5829; UV/Vis (benzene): $\lambda_{max} = 410.0$ (Soret), 431.0 (Soret), 535.5, 569.0 nm.

Procedure of $AgPF_6$-promoted coupling reaction of 1,4-phenylene-bridged porphyrin arrays: As a typical example, the synthetic procedure of the tetramer **11-Ni** is described. The 1,4-phenylene-bridged Ni^{II}-Zn^{II} porphyrin dimer **10-Ni** (12.3 mg, 0.0076 mmol) was dissolved in dry $CHCl_3$ (5.0 mL) and the reaction vessel was covered with foil. A solution of $AgPF_6$ (0.0090 mmol, 1.18 equiv) in acetonitrile was added all at once. The progress of the reaction was monitored by the analytical GPC/HPLC. After stirring for 11 h, the mixture was diluted with water, and the porphyrin products were extracted with $CHCl_3$. The combined organic extract was washed with water and dried over anhydrous Na_2SO_4. After the zinc metallation, gel-permeation chromatography (Bio-Rad Bio-Beads S-X1, eluent: toluene) afforded two major fractions that eluted in the following order: the tetramer **11-Ni** (6.3 mg, 0.0019 mmol, 51%) and the recovered **10-Ni** (4.0 mg, 0.0025 mmol, 33%). ^{1}H NMR: $\delta = 10.53$ (s, 2H; *meso*), 9.71 (d, $J = 5.0$ Hz, 2H; *β*-H), 9.59 (d, $J = 4.5$ Hz, 2H; *β*-H), 9.53 (d, $J = 4.5$ Hz, 2H; *β*-H), 9.53 (br, 2H; *meso*), 9.37 (br, 2H; *meso*), 9.26 (d, $J = 5.0$ Hz, 2H; *β*-H), 9.10 (d, $J = 5.0$ Hz, 2H; *β*-H), 8.83 (d, $J = 5.0$ Hz, 2H; *β*-H), 8.57 (t, $J = 8.5$ Hz, 8H; Ar), 8.39 (d, $J = 5.0$ Hz, 2H; *β*-H), 8.26 (d, $J = 5.0$ Hz, 2H; *β*-H), 8.21 (d, $J = 8.5$ Hz, 2H; Ar), 8.16 (s, 2H; Ar), 7.74 (s, 2H; Ar), 7.73 (d, $J = 8.0$ Hz, 4H; Ar), 7.43 (d, $J = 8.0$ Hz, 4H; Ar), 6.88 (d, $J = 8.5$ Hz, 2H; Ar), 6.85 (d, $J = 3.0$ Hz, 2H; Ar), 6.80 (dd, $J = 8.5$, 3.0 Hz, 2H; Ar), 4.21 (s, 4H; Ar-CH_2-Ar), 3.86 (s, 6H; OMe), 3.80 (s, 6H; OMe), 3.85–3.50 (m, 16H; hexyl), 2.93 (br, 6H; Me), 2.53 (br, 6H; Me), 2.18 (br, 12H; Me), 1.49 (s, 36H; *t*Bu), 2.24–0.65 (m, 88H; hexyl); MS (TOF): found 3243; calcd for $C_{206}H_{230}N_{16}Ni_2O_4Zn_2$: 3242; UV/Vis (benzene): $\lambda_{max} = 417.0$ (Soret), 451.0, 535.5, 417.0 nm.

The amounts of $AgPF_6$ and the reaction time used for the coupling reactions of the other 1,4-phenylene-bridged porphyrin arrays and the windmill porphyrin arrays are summarized in Table 1.

Windmill porphyrin hexamer 17-Ni and nonamer 18: This compound was prepared from the trimer **14-Ni** (39.1 mg, 0.0157 mmol). Separation by the recycling preparative GPC/HPLC (JAI-GEL, eluent: $CHCl_3$) gave three major fractions in the following order: a trace amount of nonamer **18** (ca.

2%), hexamer **17-Ni** (19.4 mg, 0.0039 mmol, 50%), and the recovered trimer **14-Ni** (18.5 mg, 0.0074 mmol, 47%).

Hexamer: ^{1}H NMR: $\delta = 10.67$ (s, 2H; *meso*), 9.79 (d, $J = 4.0$ Hz, 4H; β-H), 9.60 (d, $J = 4.0$ Hz, 4H; β-H), 9.53 (br, 4H; *meso*), 9.36 (br, 4H; *meso*), 9.18 (d, $J = 5.0$ Hz, 4H; β-H), 8.61 (d, $J = 8.0$ Hz, 8H; Ar), 8.52 (d, $J = 4.0$ Hz, 4H; β-H), 8.24 (d, $J = 8.0$ Hz, 8H; Ar), 7.72 (d, $J = 8.0$ Hz, 8H; Ar), 7.42 (d, $J = 8.0$ Hz, 8H; Ar), 6.88 (d, $J = 9.0$ Hz, 4H; Ar), 6.84 (d, $J = 3.0$ Hz, 4H; Ar), 6.79 (dd, $J = 9.0$, 3.0 Hz, 4H; Ar), 4.21 (s, 8H; Ar-CH_2-Ar), 3.86 (s, 12H; OMe), 3.80 (s, 12H; OMe), 3.87–3.51 (m, 32H; hexyl), 2.96 (br, 12H; Me), 2.58 (br, 12H; Me), 2.23 (br, 24H; Me), 1.93–0.63 (m, 176H; hexyl); MS (TOF): found 4985; calcd for $C_{316}H_{358}N_{24}Ni_4O_8Zn_2$: 4985; UV/Vis (benzene): $\lambda_{max} = 414.5$ (Soret), 529.5, 565.0 nm.

Nonamer 18: ^{1}H NMR: $\delta = 10.71$ (s, 2H; *meso*), 9.82 (d, $J = 4.5$ Hz, 4H; β-H), 9.64 (d, $J = 4.5$ Hz, 4H; β-H), 9.56 (br, 4H; *meso*), 9.41 (br, 4H; *meso*), 9.34 (d, $J = 4.5$ Hz, 4H; β-H), 9.33 (s, 4H; *meso*), 9.26 (d, $J = 4.5$ Hz, 4H; β-H), 8.76 (d, $J = 4.5$ Hz, 4H; β-H), 8.69 (d, $J = 8.5$ Hz, 8H; Ar), 8.65 (m, 8H; β-H, Ar), 8.32 (d, $J = 8.5$ Hz, 8H; Ar), 8.16 (d, $J = 8.0$ Hz, 4H; Ar), 7.75 (d, $J = 8.5$ Hz, 8H; Ar), 7.65 (d, $J = 8.5$ Hz, 4H; Ar), 7.44 (d, $J = 8.5$ Hz, 8H; Ar), 7.36 (d, $J = 8.5$ Hz, 4H; Ar), 6.90–6.76 (m, 18H; Ar), 4.23 (s, 8H; Ar-CH_2-Ar), 4.15 (s, 4H; Ar-CH_2-Ar), 3.87 (s, 12H; OMe), 3.87–3.46 (m, 48H; hexyl), 3.81 (s, 12H; OMe), 3.75 (s, 6H; OMe), 3.46 (s, 6H; OMe), 3.00, 2.68, 2.58, 2.56 (2br, 2s, 72H; Me), 2.36–0.62 (m, 264H; hexyl); MS (TOF): found 7476; calcd for $C_{474}H_{536}N_{36}Ni_6O_{12}Zn_3$: 7478; UV/Vis (benzene): $\lambda_{max} = 418.5$ (Soret), 474.5, 533.0, 564.5 nm.

Windmill porphyrin array 19-Ni: This compound was prepared from the trimer **15-Ni** (33.5 mg, 0.0081 mmol). Separation by the recycling preparative GPC/HPLC (JAI-GEL, eluent: $CHCl_3$) gave three major fractions in the following order: a trace amount of 15-mer **20**, decamer **19-Ni** (11.8 mg, 0.00141 mmol, 35%), and the recovered pentamer **15-Ni** (5.0 mg, 0.0012 mmol, 15%). Decamer **19-Ni**: ^{1}H NMR: $\delta = 10.69$ (s, 2H; *meso*), 9.81 (d, $J = 4.0$ Hz, 4H; β-H), 9.62 (d, $J = 4.5$ Hz, 4H; β-H), 9.56 (br, 8H; *meso*), 9.42 (br, 8H; *meso*), 9.22 (d, $J = 4.5$ Hz, 4H; β-H), 8.65 (d, $J = 8.0$ Hz, 8H; Ar), 8.55 (d, $J = 4.5$ Hz, 4H; β-H), 8.29 (d, $J = 8.0$ Hz, 8H; Ar), 8.12 (s, 16H; Ar), 7.74 (d, $J = 8.0$ Hz, 8H; Ar), 7.45 (d, $J = 8.0$ Hz, 8H; Ar), 6.90 (d, $J = 9.0$ Hz, 4H; Ar), 6.86 (d, $J = 3.0$ Hz, 4H; Ar), 6.81 (dd, $J = 9.0$, 3.0 Hz, 4H; Ar), 4.23 (s, 8H; Ar-CH_2-Ar), 3.88 (s, 12H; OMe), 3.81 (s, 12H; OMe), 3.88–3.50 (m, 64H; hexyl), 2.96 (br, 24H; Me), 2.74 (br, 24H; Me), 2.60 (br, 24H; Me), 2.25 (br, 24H; Me), 2.20–0.65 (m, 352H; hexyl); MS (TOF): found 8321; calcd for $C_{532}H_{638}N_{40}Ni_8O_8Zn_2$: 8320; UV/Vis (benzene): $\lambda_{max} = 410.0$ (Soret), 430.0 (Soret), 534.0, 567.0 nm.

Windmill porphyrin array 21-Ni: This compound was prepared from the heptamer **16-Ni** (21.7 mg, 0.00372 mmol). Separation by the recycling preparative GPC/HPLC (JAI-GEL, eluent: $CHCl_3$) gave three major fractions in the following order: trace amount of 21-mer, 14-mer **21-Ni** (3.0 mg, 0.00206 mmol, 14%), and the recovered heptamer **16-Ni**. 14-mer **21-Ni**: ^{1}H NMR: $\delta = 10.69$ (s, 2H; *meso*), 9.81 (d, $J = 4.0$ Hz, 4H; β-H), 9.62 (d, $J = 4.0$ Hz, 4H; β-H), 9.56, 9.46, 9.44 (br, 2s, 24H; *meso*), 9.22 (br, 4H; β-H), 8.67 (d, $J = 8.0$ Hz, 8H; Ar), 8.54 (br, 4H; β-H), 8.30 (d, $J = 8.0$ Hz, 8H; Ar), 8.15 (s, 16H; Ar), 8.14 (s, 16H; Ar), 7.76 (d, $J = 7.5$ Hz, 8H; Ar), 7.46 (d, $J = 7.5$ Hz, 8H; Ar), 6.91 (d, $J = 8.5$ Hz, 4H; Ar), 6.87 (d, $J = 2.5$ Hz, 4H; Ar), 6.82 (dd, $J = 8.5$, 2.5 Hz, 4H; Ar), 4.23 (s, 8H; Ar-CH_2-Ar), 3.88 (s, 12H; OMe), 3.82 (s, 12H; OMe), 3.73, 3.66 (2br, 96H; hexyl), 2.99 (br, 12H; Me), 2.62 (br, 12H; Me), 2.76, 2.27 (2s, 120H; Me), 2.20–2.08 (br, 96H; hexyl), 2.00–1.26 (br, 288H; hexyl), 1.20–0.85 (br, 144H; hexyl); MS (TOF): found 11640; calcd for $C_{748}H_{918}N_{56}Ni_{12}O_8Zn_2$: 11656; UV/Vis (benzene): $\lambda_{max} = 412.0$ (Soret), 434.0 (Soret), 535.5, 568 nm.

General procedure for the transformation of partially Ni^{II}-metallated porphyrin arrays into all Zn^{II}-metallated porphyrin arrays: Ni^{II} porphyrin was dissolved in a mixture of toluene, TFA, and 10% H_2SO_4. After heating under reflux for 2–3 h, the mixture was poured into water and the porphyrin products were extracted with toluene. The combined organic extracts were washed with water, $NaHCO_3$ (aq), and brine, and dried over Na_2SO_4. A saturated solution of Zn^{II} acetate in MeOH was added to this solution, and the mixture was refluxed for 1 h. The reaction mixture was poured into water and the porphyrin products were extracted with CH_2Cl_2. The combined organic extracts were washed with water and brine, and dried over Na_2SO_4. Separation by silica gel chromatography gave the corresponding all Zn^{II} porphyrins in a pure state. Some of ^{1}H NMR spectra of all Zn^{II}-metallated were very broad and, therefore, are not reported here.

Dimer 10-Zn: ^{1}H NMR: $\delta = 10.48$ (s, 2H; *meso*), 10.32 (s, 2H; *meso*), 9.69 (d, 2H; β-H), 9.64 (d, 2H; β-H), 9.54 (d, 2H; β-H), 9.27 (d, 2H; β-H), 8.68 (d, $J = 8.0$ Hz, 2H; Ar), 8.56 (d, $J = 8.0$ Hz, 2H; Ar), 8.19 (d, 2H; Ar), 8.02 (d, $J = 7.0$ Hz, 2H; Ar), 7.88 (s, 1H; Ar), 7.66 (d, $J = 7.0$ Hz, 2H; Ar), 7.00 (d, $J = 3.0$ Hz, 1H; Ar), 6.96 (d, $J = 8.5$ Hz, 1H; Ar), 6.88 (dd, $J = 8.5$, 3.0 Hz, 1H; Ar), 4.35 (s, 2H; Ar-CH_2-Ar), 3.96 (s, 3H; OMe), 3.90 (s, 3H; OMe), 4.19 (t, $J = 7.5$ Hz, 4H; hexyl), 4.04 (t, $J = 7.5$ Hz, 4H; hexyl), 3.20 (s, 6H; Me), 2.55 (s, 6H; Me), 2.37 (m, 4H; hexyl), 2.25 (m, 4H; hexyl), 1.90 (m, 4H; hexyl), 1.80 (m, 4H; hexyl) 1.53 (s, 18H; *t*Bu), 1.60–1.42 (m, 16H; hexyl), 1.00–0.90 (m, 12H; hexyl); MS (FAB): found 1629; calcd for $C_{103}H_{116}N_8O_2Zn_2$: 1629; UV/Vis (CH_2Cl_2): $\lambda_{max} = 409.0$ (Soret), 419.5 (Soret), 538, 572.0 nm; fluorescence (CH_2Cl_2): $\lambda_{max} = 579.4$, 629.0 nm (excitation at 540 nm).

Tetramer 11-Zn: ^{1}H NMR: $\delta = 10.58$ (s, 2H; *meso*), 10.28 (s, 2H; *meso*), 10.11 (s, 2H; *meso*), 9.78 (d, $J = 4.5$ Hz, 2H; β-H), 9.69 (d, $J = 5.0$ Hz, 2H; β-H), 9.61 (d, $J = 5.0$ Hz, 2H; β-H), 9.28 (d, $J = 4.5$ Hz, 2H; β-H), 9.26 (d, $J = 4.5$ Hz, 2H; β-H), 8.86 (d, $J = 4.5$ Hz, 2H; β-H), 8.70 (d, $J = 7.5$ Hz, 4H; Ar), 8.48 (d, $J = 4.0$ Hz, 2H; β-H), 8.45 (m, 4H; Ar-H), 8.31 (d, $J = 4.5$ Hz, 2H; β-H), 8.20 (d, $J = 7.5$ Hz, 4H; Ar), 7.95 (m, 4H; Ar), 7.76 (m, 2H; Ar), 7.54 (d, $J = 8.0$ Hz, 4H; Ar), 6.95 (d, $J = 3.0$ Hz, 2H; Ar), 6.92 (d, $J = 9.0$ Hz, 2H; Ar), 6.85 (dd, $J = 9.0$, 3.0 Hz, 2H; Ar), 4.31 (s, 4H; Ar-CH_2-Ar), 4.17 (m, 4H; hexyl), 4.00 (m, 4H; hexyl), 3.91 (s, 6H; OMe), 3.86 (m, 4H; hexyl), 3.85 (s, 6H; OMe), 3.79 (m, 4H; hexyl), 3.20 (s, 6H; Me), 2.80 (s, 6H; Me), 2.50 (s, 6H; Me), 2.46 (s, 6H; Me), 2.35 (m, 4H; hexyl), 2.21 (m, 4H; hexyl), 2.09 (m, 4H; hexyl), 2.00 (m, 4H; hexyl), 1.90 (m, 4H; hexyl), 1.77 (m, 4H; hexyl), 1.65–1.35 (m, 28H; hexyl), 1.55 (s, 36H; *t*Bu), 1.26 (m, 8H; hexyl), 1.09 (m, 4H; hexyl), 0.98 (m, 6H; hexyl), 0.94 (m, 6H; hexyl), 0.80 (m, 6H; hexyl), 0.62 (m, 6H; hexyl); MS (FAB): found 3254; calcd for $C_{206}H_{230}N_{16}O_4Zn_4$: 3255; UV/Vis ($CH_2Cl_2$): $\lambda_{max} = 413.5$ (Soret), 447.0, 546.5, 571.5 nm; fluorescence(CH_2Cl_2): $\lambda_{max} = 579$, 596, 651.2 nm (excitation at 540 nm).

Linear trimer 14-Zn: MS (TOF): found 2506; calcd for $C_{158}H_{180}N_{12}O_4Zn_3$: 2507; UV/Vis ($CH_2Cl_2$): $\lambda_{max} = 406.5$ (Soret), 424.0 (Soret), 539.0, 573.0 nm; fluorescence (CH_2Cl_2): $\lambda_{max} = 579$, 631 nm (excitation at 540 nm).

Windmill hexamer 17-Zn: ^{1}H NMR: $\delta = 10.77$ (s, 2H; *meso*), 10.29 (s, 4H; *meso*), 10.10 (s, 4H; *meso*), 9.91 (d, $J = 4.0$ Hz, 4H; β-H), 9.79 (d, $J = 4.0$ Hz, 4H; β-H), 9.40 (d, $J = 4.0$ Hz, 4H; β-H), 8.77 (m, 8H; Ar), 8.68 (d, $J = 4.0$ Hz, 4H; β-H), 8.50 (m, 8H; Ar), 7.94 (d, $J = 8.5$ Hz, 8H; Ar), 7.53 (d, $J = 8.5$ Hz, 8H; Ar), 6.94 (d, $J = 3.0$ Hz, 4H; Ar), 6.92 (d, $J = 8.0$ Hz, 4H; Ar), 6.83 (dd, $J = 8.0$, 3.0 Hz, 4H; Ar), 4.30 (s, 8H; Ar-CH_2-Ar), 4.20 (m, 8H; hexyl), 4.01 (m, 8H; hexyl), 3.91 (s, 12H; OMe), 3.84 (s, 12H; OMe), 3.90–3.80 (m, 16H; hexyl), 3.25 (s, 12H; Me), 2.85 (s, 12H; Me), 2.50 (s, 12H; Me), 2.44 (s, 12H; Me), 2.38–0.58 (m, 128H; hexyl), 1.01 (t, $J = 7.5$ Hz, 12H; hexyl), 0.94 (t, $J = 7.0$ Hz, 12H; hexyl), 0.77 (t, $J = 7.0$ Hz, 12H; hexyl), 0.59 (t, $J = 7.5$ Hz, 12H; hexyl); MS (FAB): found 5018; calcd for $C_{316}H_{358}N_{24}O_8Zn_6$: 5012; UV/Vis ($CH_2Cl_2$): $\lambda_{max} = 410.5$ (Soret), 423.5 (Soret), 541.5, 573.0 nm; fluorescence (CH_2Cl_2): $\lambda_{max} = 580$, 596, 650 nm (excitation at 540 nm).

Linear pentamer 15-Zn: MS (TOF): found 4180; calcd for $C_{266}H_{320}N_{20}O_4Zn_5$: 4188; UV/Vis ($CH_2Cl_2$): $\lambda_{max} = 409.5$ (Soret), 427.5 (Soret), 539.5, 571.0 nm; fluorescence (CH_2Cl_2): $\lambda_{max} = 579$, 632 nm (excitation at 540 nm).

Windmill decamer 19-Zn: MS (TOF): found 8385; calcd for $C_{532}H_{638}N_{40}O_8Zn_{10}$: 8375; UV/Vis ($CH_2Cl_2$): $\lambda_{max} = 412.5$ (Soret), 429.0 (Soret), 545.5, 575.0 nm; Fluorescence (CH_2Cl_2): $\lambda_{max} = 582.4$, 645.8, 701 nm (excitation at 540 nm).

1,4-Phenylene-bridged Ni^{II}-Zn^{II}-Ni^{II} porphyrin trimer 24-Ni: This compound was prepared from the reaction of Ni^{II} formyl-substituted porphyrin (0.474 mmol) and 2,2′-dipyrrylmethane **8** by the procedure used for the preparation of **14-Ni**. Yield was 30% (192 mg, 0.0708 mmol). ^{1}H NMR: $\delta = 10.45$ (s, 2H; *meso*), 9.62 (d, $J = 4.5$ Hz, 4H; β-H), 9.59 (s, 4H; *meso*), 9.49 (d, $J = 4.0$ Hz, 4H; β-H), 8.58 (d, $J = 7.5$ Hz, 4H; Ar), 8.36 (d, $J = 7.0$ Hz, 4H; Ar), 7.12 (s, 4H; Ar), 6.86 (s, 2H; Ar), 4.09 (t, $J = 7.0$ Hz, 8H; octyl), 3.89 (m, 8H; hexyl), 3.77 (m, 8H; hexyl), 2.98 (s, 12H; Me), 2.52 (s, 12H; Me), 2.22 (m, 8H; hexyl), 2.13 (m, 8H; hexyl), 1.87, 1.81, 1.72 (3m, 3 × 8H; hexyl, octyl), 1.59–1.32 (m, 72H; hexyl, octyl), 1.01 (t, $J = 7.5$ Hz, 12H; hexyl), 0.99 (t, $J = 7.0$ Hz, 12H; hexyl), 0.91 (t, $J = 7.5$ Hz, 12H; octyl); MS (TOF): found 2707; calcd for $C_{172}H_{224}N_{12}Ni_2O_4Zn$: 2706; UV/Vis ($CH_2Cl_2$): $\lambda_{max} = 405$, 422, 535, 563 nm.

0947-6539/00/0617-3268 $ 17.50+.50/0 *Chem. Eur. J.* **2000**, *6*, No. 17

Windmill porphyrin array 25-Ni and grid porphyrin array 26-Ni: These compounds were prepared from the trimer **24-Ni** (0.050 mmol). Separation by the recycling preparative GPC/HPLC (JAI-GEL, eluent: $CHCl_3$) gave three major fractions in the following order: a small amount of nonamer **26-Ni**, hexamer **25-Ni** (30.5 mg, 22%), and the recovered trimer **24-Ni** (83 mg, 62%).

Hexamer 25-Ni: ^{1}H NMR: $\delta = 10.63$ (s, 2H; *meso*), 9.77 (d, $J = 4.5$ Hz, 4H; β-H), 9.59 (d, $J = 4.0$ Hz, 4H; β-H), 9.56 (br, 4H; *meso*), 9.41 (br, 4H; *meso*), 9.18 (d, $J = 5.0$ Hz, 4H; β-H), 8.64 (d, $J = 8.0$ Hz, 8H; Ar), 8.50 (d, $J = 5.0$ Hz, 4H; β-H), 8.27 (d, $J = 8.0$ Hz, 8H; Ar), 7.03 (d, $J = 2.5$ Hz, 8H; Ar), 6.80 (s, 4H; Ar), 4.02 (t, $J = 7.0$ Hz, 16H; octyl), 3.89 (br, 8H; hexyl), 3.73 (br, 8H; hexyl), 3.62 (br, 8H; hexyl), 3.54 (br, 8H; hexyl), 2.99 (br, 12H; Me), 2.61 (br, 12H; Me), 2.45 (br, 12H; Me), 2.42 (br, 12H; Me), 2.21 (m, 8H; hexyl), 2.07 (m, 8H; hexyl), 1.97 (m, 8H; hexyl), 1.85 (m, 8H; hexyl), 1.81 (m, 16H; octyl), 1.78–0.85 (m, 248H; hexyl, octyl); MS (TOF): found 5400; calcd for $C_{344}H_{446}N_{24}Ni_4O_8Zn_2$: 5411; UV/Vis ($CH_2Cl_2$): $\lambda_{max} =$ 411, 421, 532, 560 nm.

Nonamer 26-Ni: ^{1}H NMR: $\delta = 10.67$ (s, 2H; *meso*), 9.80 (d, $J = 4.5$ Hz, 4H; β-H), 9.62 (d, $J = 4.0$ Hz, 4H; β-H), 9.56 (br, 4H; *meso*), 9.43 (br, 4H; *meso*), 9.34 (s, d, $J = 5.0$ Hz, 8H; *meso*, β-H), 9.25 (d, $J = 4.5$ Hz, 4H; β-H), 8.75 (d, $J = 4.5$ Hz, 4H; β-H), 8.69 (d, $J = 8.5$ Hz, 8H; Ar), 8.64 (m, 8H; β-H, Ar), 8.32 (d, $J = 8.0$ Hz, 8H; Ar), 8.16 (d, $J = 8.0$ Hz, 4H; Ar), 7.02 (d, $J = 2.5$ Hz, 8H; Ar), 6.92 (d, $J = 2.5$ Hz, 4H; Ar), 6.79 (s, 4H; Ar), 6.71 (s, 2H; Ar), 4.01 (t, $J = 6.5$ Hz, 16H; octyl), 3.93 (t, $J = 7.0$ Hz, 8H; octyl), 3.91–3.44 (m, 48H; hexyl), 3.06 (br, 12H; Me), 2.69 (br, 12H; Me), 2.58 (s, 12H; Me), 2.50 (br, 24H; Me), 2.35, (s, 12H; Me), 2.21–0.62 (m, 444H; hexyl, octyl); MS (TOF): found 8131; calcd for $C_{516}H_{668}N_{36}Ni_6O_{12}Zn_3$: 8115; UV/Vis ($CH_2Cl_2$): $\lambda_{max} = 412$, 471, 533, 563 nm.

Grid porphyrin arrays 27, 28, 29, 30, and 31: The grid porphyrin arrays **27**, **28**, and **29** were prepared from the windmill hexamer **25-Ni** (27 mg, 0.0050 mmol). Separation by the recycling preparative GPC/HPLC (JAI-GEL, eluent: $CHCl_3$) gave four major fractions in the following order: a small amount of 24-mer **29**, 18-mer **28**, 12-mer **27** (6.7 mg, 25%), and the recovered hexamer **25-Ni** (9.4 mg, 35%). The grid porphyrin 12-mer **27** was subjected to the same coupling conditions and the subsequent separation by the recycling preparative GPC/HPLC (JAI-GEL, eluent: $CHCl_3$) gave the 24-mer **29**, 36-mer **30**, and 48-mer **31**. The yields were not determined, but these large porphyrin arrays could be characterized by MALDI-TOF MS, UV/Vis absorption spectra (Figure 6), and GPC/HPLC retention times (Table 2 and Figure 5).

12-mer 27: ^{1}H NMR: $\delta = 10.68$ (s, 2H; *meso*), 9.82 (d, $J = 4.5$ Hz, 4H; β-H), 9.64 (d, $J = 4.0$ Hz, 4H; β-H), 9.59 (br, 4H; *meso*), 9.46 (br, 4H; *meso*), 9.41 (d, $J = 4.5$ Hz, 4H; β-H), 9.39 (m, 8H; *meso*), 9.36 (d, $J = 4.5$ Hz, 4H; β-H), 9.28 (d, $J = 4.0$ Hz, 4H; β-H), 8.86 (d, $J = 4.0$ Hz, 4H; β-H), 8.78 (d, $J = 4.0$ Hz, 4H; β-H), 8.73 (m, 16H; Ar), 8.65 (d, $J = 5.0$ Hz, 4H; β-H), 8.34 (d, $J = 8.0$ Hz, 8H; Ar), 8.24 (d, $J = 8.0$ Hz, 8H; Ar), 7.04 (d, $J = 2.5$ Hz, 8H; Ar), 6.96 (d, $J = 2.5$ Hz, 8H; Ar), 6.80 (s, 4H; Ar), 6.74 (s, 4H; Ar), 4.03 (t, $J = 7.0$ Hz, 16H; octyl), 3.97 (t, $J = 6.5$ Hz, 16H; octyl), 4.04–3.50, 3.03–1.21, 1.03–0.69 (m, 704H; Me, hexyl, octyl), 0.85 (t, $J = 7.0$ Hz, 24H; octyl), 0.80 (t, $J = 7.0$ Hz, 24H; octyl); MS (TOF): found 10822; calcd for $C_{688}H_{890}N_{48}Ni_8O_{16}Zn_4$: 10820; UV/Vis ($CH_2Cl_2$): $\lambda_{max} = 413$, 483, 532, 566 nm.

18-mer 28: Mass (TOF): found 16211; calcd for $C_{1032}H_{1334}N_{72}Ni_{12}O_{24}Zn_6$: 16229; UV/Vis ($CH_2Cl_2$): $\lambda_{max} = 412$, 494, 531, 567 nm.

24-mer 29: Mass (TOF): found 21466; calcd for $C_{1376}H_{1778}N_{96}Ni_{16}O_{32}Zn_8$: 21638; UV/Vis ($CH_2Cl_2$): $\lambda_{max} = 412$, 500, 567 nm.

36-mer 30: Mass (TOF): found 32276; calcd for $C_{2064}H_{2666}N_{144}Ni_{24}O_{48}Zn_{12}$: 32456.

48-mer 31: Mass (TOF): found 43321; calcd for $C_{2752}H_{3554}N_{192}Ni_{32}O_{64}Zn_{16}$: 43274.

1,4-Phenylene-bridged Ni^{II}-Ni^{II}-Zn^{II}-Ni^{II}-Ni^{II} porphyrin pentamer 32: This compound was prepared from the reaction of Ni^{II} formyl-substituted diporphyrin (0.148 mmol) and 2,2′-dipyrrylmethane **8** by the procedure used for the preparation of **14-Ni**. Yield was 24% (76.3 mg, 0.0174 mmol). ^{1}H NMR: $\delta = 10.56$ (s, 2H; *meso*), 9.70 (d, $J = 4.5$ Hz, 4H; β-H), 9.60 (s, 4H; *meso*), 9.55 (d, $J = 4.5$ Hz, 4H; β-H), 9.47 (s, 4H; *meso*), 8.62 (d, $J = 7.0$ Hz, 4H; Ar), 8.38 (d, $J = 7.5$ Hz, 4H; Ar), 8.20 (m, 8H; Ar), 7.05 (d, $J = 2.5$ Hz, 4H; Ar), 6.81 (s, 2H; Ar), 4.04 (t, $J = 6.5$ Hz, 8H; octyl), 3.90 (br, 8H; hexyl), 3.82 (br, 8H; hexyl), 3.76 (br, 8H; hexyl), 3.69 (br, 8H; hexyl), 2.98 (br, 12H; Me), 2.84 (br, 12H; Me), 2.81 (br, 12H; Me), 2.45 (br, 12H; Me), 2.24–2.04 (m, 32H; hexyl), 1.85–1.26 (m, 144H; hexyl, octyl), 1.01–0.88 (m, 48H; hexyl), 0.87 (t, $J = 6.5$ Hz, 12H; octyl); MS (TOF): found 4365; calcd for $C_{280}H_{364}N_{20}Ni_4O_4Zn$: 4374; UV/Vis ($CH_2Cl_2$): $\lambda_{max} = 405$, 427, 534, 567 nm.

Windmill porphyrin array 33 and grid porphyrin arrays 34, 35, and 36: These compounds were prepared from the pentamer **32** (44 mg, 0.010 mmol). Separation by the recycling preparative GPC/HPLC (JAI-GEL, eluent: $CHCl_3$) gave four major fractions in the following order: a small amount of 20-mer **35**, 15-mer **34** (3.2 mg, 7%), decamer **33** (12.1 mg, 28%), and the recovered pentamer **32** (5.0 mg, 11%). The grid porphyrin 30-mer **36** was also prepared by the coupling of 10-mer **33**.

Decamer 33: ^{1}H NMR: $\delta = 10.65$ (s, 2H; *meso*), 9.79 (d, $J = 4.5$ Hz, 4H; β-H), 9.61 (d, $J = 4.0$ Hz, 4H; β-H), 9.59 (br, 4H; *meso*), 9.46 (s, 8H; *meso*), 9.44 (br, 4H; *meso*), 9.20 (d, $J = 4.5$ Hz, 4H; β-H), 8.68 (d, $J = 7.5$ Hz, 8H; Ar), 8.53 (d, $J = 4.5$ Hz, 4H; β-H), 8.31 (d, $J = 7.5$ Hz, 8H; Ar), 8.15 (m, 16H; Ar), 7.05 (d, $J = 2.5$ Hz, 8H; Ar), 6.82 (s, 4H; Ar), 4.05 (t, $J = 6.5$ Hz, 16H; octyl), 4.03–2.06, 1.85–1.20, 1.10–0.68 (m, 608H; Me, hexyl, octyl), 0.88 (t, $J = 7.0$ Hz, 24H; octyl); MS (TOF): found 8741; calcd for $C_{560}H_{726}N_{40}Ni_8O_8Zn_2$: 8746; UV/Vis ($CH_2Cl_2$): $\lambda_{max} = 408$ (sh), 427, 533, 566 nm.

15-mer 34: Mass (TOF): found 13038; calcd for $C_{840}H_{1088}N_{60}Ni_{12}O_{12}Zn_3$: 13119; UV/Vis ($CH_2Cl_2$): $\lambda_{max} = 405$ (sh), 428, 534, 567 nm.

20-mer 35: Mass (TOF): found 17426; calcd for $C_{1120}H_{1450}N_{80}Ni_{16}O_{16}Zn_4$: 17491; UV/Vis ($CH_2Cl_2$): $\lambda_{max} = 407$ (sh), 426, 484, 534, 568 nm.

30-mer 36: Mass: not detected; calcd for $C_{1680}H_{2174}N_{120}Ni_{24}O_{24}Zn_6$: 26236; UV/Vis ($CH_2Cl_2$): $\lambda_{max} = 422$, 496, 533, 568 nm.

1,4-Phenylene-bridged Zn^{II}-Zn^{II}-Zn^{II} porphyrin trimer 24-Zn: This compound was prepared from the reaction of formyl-substituted porphyrin (0.500 mmol) and 2,2′-dipyrrylmethane **8** by the procedure used for the preparation of **14-Ni**. Yield was 37% (252 mg, 0.0925 mmol). ^{1}H NMR: $\delta = 10.53$ (s, 2H; *meso*), 10.30 (s, 4H; *meso*), 9.71 (d, $J = 4.0$ Hz, 4H; β-H), 9.64 (d, $J = 3.5$ Hz, 4H; β-H), 8.69 (d, $J = 7.5$ Hz, 4H; Ar), 8.57 (d, $J = 6.5$ Hz, 4H; Ar), 7.31 (d, $J = 2.0$ Hz, 4H; Ar), 6.96 (m, 2H; Ar), 4.14 (t, $J = 7.5$ Hz, 8H; octyl), 4.16 (br, 8H; hexyl), 4.05 (br, 8H; hexyl), 3.22 (s, 12H; Me), 2.73 (s, 12H; Me), 2.38 (br, 8H; hexyl), 2.27 (br, 8H; hexyl), 1.94–1.26 (m, 96H; hexyl, octyl), 0.99 (t, $J = 7.5$ Hz, 12H; hexyl), 0.96 (t, $J = 7.5$ Hz, 12H; hexyl), 0.88 (t, $J = 7.0$ Hz, 12H; octyl); MS (TOF): found 2720; calcd for $C_{172}H_{224}N_{12}O_4Zn_3$: 2720; UV/Vis (THF): $\lambda_{max} = 410$, 429, 547, 579 nm; fluorescence (THF): $\lambda_{max} = 585$, 540 nm (excitation at 540 nm).

1,4-Phenylene-bridged Cu^{II}-Zn^{II}-Cu^{II} porphyrin trimer 24-Cu: This compound was prepared from the reaction of Cu^{II} formyl-substituted porphyrin (0.470 mmol) and 2,2′-dipyrrylmethane **8** by the procedure used for the preparation of **14-Ni**. Yield was 42% (267 mg, 0.0981 mmol). Mass (FAB): found 2716; calcd for $C_{172}H_{224}Cu_2N_{12}O_4Zn$: 2716; UV/Vis (THF): $\lambda_{max} =$ 406, 425, 537, 567 nm.

Windmill porphyrin array 25-Zn: This compound was prepared from the trimer **24-Zn** (202 mg, 0.0743 mmol). Separation by the recycling preparative GPC/HPLC (JAI-GEL, eluent: $CHCl_3$) gave three major fractions in the following order: nonamer **26-Zn** (7.0 mg, 3%), hexamer **25-Zn** (96.1 mg, 0.0177 mmol, 48%), and the recovered trimer **24-Zn** (85.7 mg, 0.0315 mmol, 42%).

Hexamer 25-Zn: ^{1}H NMR: $\delta = 10.72$ (s, 2H; *meso*), 10.30 (s, 4H; *meso*), 10.12 (s, 4H; *meso*), 9.88 (d, $J = 4.0$ Hz, 4H; β-H), 9.77 (d, $J = 4.5$ Hz, 4H; β-H), 9.37 (d, $J = 4.0$ Hz, 4H; β-H), 8.77 (d, $J = 8.0$ Hz, 8H; Ar), 8.66 (d, $J = 5.0$ Hz, 4H; β-H), 8.50 (d, $J = 8.0$ Hz, 8H; Ar), 7.23 (d, $J = 2.5$ Hz, 8H; Ar), 6.89 (s, 4H; Ar), 4.21 (br, 8H; hexyl), 4.07 (t, $J = 6.5$ Hz, 16H; octyl), 4.06 (br, 8H; hexyl), 3.90 (br, 8H; hexyl), 3.83 (br, 8H; hexyl), 3.27 (s, 12H; Me), 2.87 (s, 12H; Me), 2.68 (s, 12H; Me), 2.63 (s, 12H; Me), 3.36–1.07 (m, 224H; hexyl, octyl), 1.02 (t, $J = 7.5$ Hz, 12H; hexyl), 0.95 (t, $J = 7.5$ Hz, 12H; hexyl), 0.81 (t, $J = 7.5$ Hz, 24H; octyl), 0.78 (t, $J = 7.5$ Hz, 12H; hexyl), 0.60 (t, $J = 7.5$ Hz, 12H; hexyl); MS (TOF): found 5435; calcd for $C_{344}H_{446}N_{24}O_8Zn_6$: 5438; UV/Vis (THF): $\lambda_{max} = 416$, 428, 548 nm; fluorescence (THF): $\lambda_{max} = 644$ nm (excitation at 540 nm).

Nonamer 26-Zn: ^{1}H NMR: $\delta = 10.79$ (s, 2H; *meso*), 10.35 (s, 4H; *meso*), 10.17 (s, 4H; *meso*), 10.09 (s, 4H; *meso*), 9.94 (d, $J = 4.5$ Hz, 4H; β-H), 9.84 (d, $J = 4.5$ Hz, 4H; β-H), 9.57 (d, $J = 4.5$ Hz, 4H; β-H), 9.49 (d, $J = 5.0$ Hz, 4H; β-H), 8.94 (d, $J = 4.0$ Hz, 4H; β-H), 8.87 (d, $J = 8.0$ Hz, 8H; Ar), 8.85 (d, $J = 7.0$ Hz, 4H; Ar), 8.81 (d, $J = 4.0$ Hz, 4H; β-H), 8.61 (d, $J = 8.0$ Hz, 8H; Ar), 8.45 (d, $J = 7.0$ Hz, 4H; Ar), 7.18 (s, 8H; Ar), 7.17 (s, 4H; Ar), 6.92

(s, 4H; Ar), 6.83 (s, 2H; Ar), 4.11 (t, $J = 6.5$ Hz, 16H; octyl), 4.01 (t, $J = 6.5$ Hz, 8H; octyl), 4.25 – 3.86 (br, 48H; hexyl), 3.32 (s, 12H; Me), 3.02 (s, 12H; Me), 2.91 (s, 12H; Me), 2.71 (s, 12H; Me), 2.65 (s, 12H; Me), 2.58 (s, 12H; Me), 2.80 – 1.16 (m, 336H; hexyl, octyl), 1.14 – 0.61 (m, 108H; hexyl, octyl); MS (TOF): found 8145; calcd for $C_{516}H_{668}N_{36}O_{12}Zn_9$: 8156; UV/Vis (THF): $\lambda_{max} = 417, 477, 548, 575$ nm; fluorescence (THF): $\lambda_{max} = 637, 671$ nm (excitation at 540 nm).

Windmill porphyrin array 25-Cu: This compound was prepared from the trimer **24-Cu** (222.3 mg, 0.0818 mmol). Separation by the recycling preparative GPC/HPLC (JAI-GEL, eluent: $CHCl_3$) gave three major fractions in the following order: nonamer **26-Cu** (18 mg, 8%), hexamer **25-Cu** (109.4 mg, 0.0201 mmol, 46%), and the recovered trimer **24-Cu** (74.8 mg, 0.0275 mmol, 32%).

Hexamer 25-Cu: MS (TOF): found 5436; calcd for $C_{344}H_{446}Cu_4N_{24}O_8Zn_2$: 5430; UV/Vis (THF): $\lambda_{max} = 410, 537, 565$ nm.

Nonamer 26-Cu: MS (TOF): found 8154; calcd for $C_{516}H_{668}Cu_6N_{36}O_{12}Zn_3$: 8145; UV/Vis (THF): $\lambda_{max} = 409, 478, 534, 568$ nm.

1,4-Phenylene-bridged porphyrin trimer 37: This compound was prepared from the reaction of 4-formylphenyl-porphyrin (0.436 mmol) and 2,2′-dipyrrylmethane by the procedure used for the preparation of **14-Ni**. Yield was 22% (110 mg, 0.0482 mmol). ^{1}H NMR: $\delta = 10.62$ (s, 2H; *meso*), 10.36 (s, 4H; *meso*), 9.77 (d, $J = 4.5$ Hz, 4H; β-H), 9.70 (d, $J = 4.0$ Hz, 4H; β-H), 8.73 (d, $J = 7.5$ Hz, 4H; Ar), 8.60 (d, $J = 8.0$ Hz, 4H; Ar), 7.32 (d, $J = 2.5$ Hz, 4H; Ar), 6.97 (m, 2H; Ar), 4.26 (m, 8H; ethyl), 4.15 (m, 16H; octyl, ethyl), 3.26 (s, 12H; Me), 2.75 (s, 12H; Me), 1.99 (t, $J = 8.0$ Hz, 12H; ethyl), 1.88 (m, 12H, 8H; ethyl, octyl), 1.53 (m, 8H; octyl), 1.40 – 1.20 (m, 32H; octyl), 0.88 (t, $J = 7.5$ Hz, 12H; octyl); MS (FAB): found 2271; calcd for $C_{140}H_{160}N_{12}O_4Zn_3$: 2271.

Windmill porphyrin hexamer 38: This compound was prepared from the trimer **37** (10.8 mg, 0.00476 mmol). Separation by the chromatography on a silica gel column (eluent; CH_2Cl_2/n-hexane) gave **38** (0.9 mg, 8%) and the recovered trimer **37**. ^{1}H NMR: $\delta = 10.77$ (s, 2H; *meso*), 10.32 (s, 4H; *meso*), 10.13 (s, 4H; *meso*), 9.90 (d, $J = 4.0$ Hz, 4H; β-H), 9.80 (d, $J = 5.0$ Hz, 4H; β-H), 9.41 (d, $J = 4.5$ Hz, 4H; β-H), 8.80 (d, $J = 8.5$ Hz, 8H; Ar), 8.68 (d, $J = 3.5$ Hz, 4H; β-H), 8.52 (d, $J = 9.0$ Hz, 8H; Ar), 7.36 (s, 8H; Ar), 6.90 (s, 4H; Ar), 4.27 (m, 8H; ethyl), 4.08 (t, $J = 6.5$ Hz, 16H; octyl), 4.09 (m, 8H; ethyl), 3.95 (m, 8H; ethyl), 3.88 (m, 8H; ethyl), 3.28 (s, 12H; Me), 2.89 (s, 12H; Me), 2.69 (s, 12H; Me), 2.64 (s, 12H; Me), 1.98 (t, $J = 8.0$ Hz, 12H; ethyl), 1.84 (m, 12H, 16H; ethyl, octyl), 1.69 (t, $J = 7.5$ Hz, 12H; ethyl), 1.60 (t, $J = 8.0$ Hz, 12H; ethyl), 1.55 – 1.25 (m, 80H; octyl), 0.98 – 0.75 (m, 24H; octyl); MS (TOF): found 4538; calcd for $C_{280}H_{318}N_{24}O_8Zn_6$: 4540; UV/Vis (THF): $\lambda_{max} = 416$, 428, 548 nm; fluorescence (THF): $\lambda_{max} = 644$ nm (excitation at 540 nm).

Nitration of the porphyrin trimer 37: The porphyrin trimer **37** (10.7 mg, 0.0047 mmol) was dissolved in dry $CHCl_3$ (5 mL), and the reaction vessel was covered with foil. A solution of $AgNO_2$ (0.010 mmol) in acetonitrile was added all at once. After stirring for 6 h, the mixture was diluted with water, and the porphyrin products were extracted with $CHCl_3$. The combined extract was washed with water and dried over anhydrous Na_2SO_4. After the zinc metallation, chromatography on a silica gel column (eluent; CH_2Cl_2/n-hexane) gave mononitrated porphyrin **39** (3.2 mg, 0.0014 mmol, 30%) and dinitrated porphyrin **40** (2.3 mg, 0.98 μmol, 21%) with the recovery of **37** (1.7 mg, 0.77 μmol, 16%).

Mononitrated porphyrin 39: ^{1}H NMR: $\delta = 10.56$ (s, 2H; *meso*), 10.35 (s, 2H; *meso*), 10.14 (s, 1H; *meso*), 9.74 (d, $J = 4.5$ Hz, 2H; β-H), 9.72 (d, $J = 4.0$ Hz, 2H; β-H), 9.69 (d, $J = 4.0$ Hz, 2H; β-H), 9.62 (d, $J = 3.0$ Hz, 2H; β-H), 8.73 (dd, $J = 7.5$ Hz, 4H; Ar), 8.60 (d, $J = 8.0$ Hz, 2H; Ar), 8.57 (d, $J = 7.5$ Hz, 2H; Ar), 7.33 (d, $J = 2.5$ Hz, 2H; Ar), 7.29 (t, $J = 2.0$ Hz, 2H; Ar), 6.97 (m, 1H; Ar), 6.95 (m, 1H; Ar), 4.25 (m, 2H; ethyl), 4.17 – 4.11 (m, 2 × 8H; octyl, ethyl), 3.99 (m, 2H; ethyl), 3.74 (m, 2H; ethyl), 3.58 (m, 2H; ethyl), 3.25 (s, 6H; Me), 3.08 (s, 3H; Me), 3.05 (s, 3H; Me), 2.76 (s, 6H; Me), 2.60 (s, 3H; Me), 2.57 (s, 3H; Me), 1.98 (t, $J = 7.5$ Hz, 8H; octyl), 1.92 – 1.86 (m, 12H, 6H; octyl, ethyl), 1.77 (t, $J = 7.5$ Hz, 3H; ethyl) 1.63 (t, $J = 7.0$ Hz, 3H; ethyl), 1.53 – 1.26 (m, 40H; octyl), 0.87 (m, 12H; octyl); MS (TOF): found 2318; calcd for $C_{140}H_{159}N_{13}O_6Zn_3$: 2316.

Dinitrated porphyrin 40: ^{1}H NMR: $\delta = 10.57$ (s, 2H; *meso*), 10.14 (s, 2H; *meso*), 9.72 (br m, 4H; β-H), 9.62 (br m, 4H; β-H), 8.73 (d, $J = 8.0$ Hz, 4H; Ar), 8.57 (d, $J = 7.5$ Hz, 4H; Ar), 7.29 (d, $J = 2.5$ Hz, 4H; Ar), 6.95 (m, 2H; Ar), 4.16 (t, $J = 6.5$ Hz, 8H; octyl), 4.13 (m, 4H; ethyl), 3.98 (m, 4H; ethyl), 3.72 (m, 4H; ethyl), 3.58 (m, 4H; ethyl), 3.08 (s, 6H; Me), 3.05 (s, 6H; Me), 2.59 (s, 6H; Me), 2.57 (s, 6H; Me), 1.92 – 1.87 (m, 12H, 8H; octyl, ethyl), 1.77 (t, $J = 7.5$ Hz, 6H; ethyl), 1.63 (t, $J = 7.5$ Hz, 6H; ethyl), 1.53 – 1.11 (m, 40H; octyl), 0.87 (m, 12H; octyl); MS (TOF): found 2362; calcd for $C_{140}H_{158}N_{14}O_8Zn_3$: 2361.

Acknowledgement

This work was supported by Grant-in-Aids for Scientific Research (No.11136221 and No. 11223205) from the Ministry of Education, Science, Sports, and Culture of Japan, and by CREST (Core Research for Evolutional Science and Technology) of Japan Science and Technology Corporation (JST).

[1] a) R. E. Martin, F. Diederich, *Angew. Chem.* **1999**, *111*, 1440 – 1469; *Angew. Chem. Int. Ed.* **1999**, *38*, 1350 – 1377; b) P. F. H. Schewab, M. D. Levin, J. Michl, *Chem. Rev.* **1999**, *99*, 1863 – 1933; c) M. G. Vicente, L. Jaquinod, K. M. Smith, *Chem. Commun.* **1999**, 1771 – 1782.

[2] a) R. W. Wagner, J. S. Lindsey, *J. Am. Chem. Soc.* **1994**, *116*, 9759 – 9760; b) R. W. Wagner, J. S. Lindsey, J. Serth, V. Palaniappan, D. F. Bocian, *J. Am. Chem. Soc.* **1996**, *118*, 3996 – 3997.

[3] M. P. Debreczeny, W. A. Svec, M. R. Wasielewski, *Science* **1996**, *274*, 584 – 587.

[4] a) S. Prathapan, T. E. Johnson, J. S. Lindsey, *J. Am. Chem. Soc.* **1993**, *115*, 7519 – 7520; b) R. W. Wagner, T. E. Johnson, J. S. Lindsey, *J. Am. Chem. Soc.* **1996**, *118*, 11166 – 11180; c) J.-S. Hsiao, B. P. Krueger, R. W. Wagner, T. E. Johnson, J. K. Delaney, D. C. Mauzerall, G. R. Fleming, J. S. Lindsey, D. F. Bocian, R. J. Donohoe, *J. Am. Chem. Soc.* **1996**, *118*, 11181 – 11193; d) J. Seth, V. Palaniappan, R. W. Wagner, T. E. Johnson, J. S. Lindsey, D. F. Bocian, *J. Am. Chem. Soc.* **1996**, *118*, 11194 – 11207.

[5] a) M. R. Wasielewski, *Chem. Rev.* **1992**, *92*, 435 – 461; b) D. Gust, T. A. Moore, A. L. Moore, *Acc. Chem. Res.* **1993**, *26*, 198 – 205; c) H. Kurreck, M. Huber, *Angew. Chem.* **1995**, 107, 929 – 947; *Angew. Chem. Int. Ed. Engl.* **1995**, *34*, 849 – 866; d) A. Osuka, N. Mataga, T. Okada, *Pure Appl. Chem.* **1997**, *69*, 797 – 802; e) G. Steinberg-Yfrach, P. A. Liddell, S.-C. Hung, A. L. Moore, D. Gust, T. A. Moore, *Nature* **1997**, *385*, 239 – 241; f) G. Steinberg-Yfrach, J.-L. Rigaud, E. N. Durantini, A. L. Moore, D. Gust, T. A. Moore, *Nature* **1998**, *392*, 479 – 482; g) A. Osuka, S. Nakajima, K. Maruyama, N. Mataga, T. Asahi, I. Yamazaki, Y. Nishimura, T. Ohno, K. Nozaki, *J. Am. Chem. Soc.* **1993**, *115*, 4577 – 4589.

[6] a) M. D. Ward, *Chem. Soc. Rev.* **1997**, *26*, 365 – 375; b) T. Hayashi, H. Ogoshi, *Chem. Soc. Rev.* **1997**, *26*, 355 – 364.

[7] a) A. Osuka, N. Tanabe, R.-P. Zhang, K. Maruyama, *Chem. Lett.* **1993**, 1505 – 1508; b) A. Osuka, N. Tanabe, S. Nakajima, K. Maruyama, *J. Chem. Soc. Perkin Trans. 2* **1996**, 199 – 203; c) J. L. Sessler, V. L. Capuano, *Angew. Chem.* **1990**, *102*, 1162 – 1164; *Angew. Chem. Int. Ed. Engl.* **1990**, *29*, 1134 – 1136; d) J. L. Sessler,V. L. Capuano, A. Harriman, *J. Am. Chem. Soc.* **1993**, *115*, 4618 – 4628.

[8] a) V. S.-Y. Lin, S. G. DiMagno, M. J. Therien, *Science* **1994**, *264*, 1105 – 1111; b) V. S.-Y. Lin, M. J. Therien, *Chem. Eur. J.* **1995**, *1*, 645 – 651; c) R. Kumble, S. Palese, V. S.-Y. Lin, M. J. Therien, R. M. Hochstrasser, *J. Am. Chem. Soc.* **1998**, *120*, 11489 – 11498; d) P. L. Taylor, A. P. Wylie, J. Huuskonen, H. L. Anderson, *Angew. Chem.* **1998**, *110*, 1033 – 1037; *Angew. Chem. Int. Ed.* **1998**, *37*, 986 – 989; e) P. N. Taylor, J. Huuskonen, G. Rumbles, R. T. Aplin, E. Williams, H. L. Anderson, *Chem. Commun.* **1998**, 909 – 910; f) B. Jiang, S.-W. Y. Yang. D. C. Barbini, W. E. Jones, Jr., *Chem. Commun.* **1998**, 213 – 214.

[9] a) G. M. Dubowchik, A. D. Hamilton, *J. Chem. Soc. Chem. Commun.* **1987**, 293 – 295; b) R. W. Wagner, J. Seth, S. I. Yang, D. Kim, D. F. Bocian, D. Holten, J. S. Lindsey, *J. Org. Chem.* **1998**, *63*, 5042 – 5049; c) J. Li, A. Ambroise, S. I. Yang, J. R. Diers, J. Seth, C. R. Wack, D. F. Bocian, D. Holten, J. S. Lindsey, *J. Am. Chem. Soc.* **1999**, *121*, 8927 – 8940; d) O. Mongin, A. Schuwey, M.-A. Vallot, A. Gossauer, *Tetrahedron Lett.* **1999**, *40*, 8347 – 8350.

[10] a) C. M. Drain, J.-M. Lehn, *J. Chem. Soc. Chem. Commun.* **1994**, 2313 – 2314; b) P. J. Stang, J. Fan, B. Olenyuk, *Chem. Commun.* **1997**, 1453 – 1454.

  0947-6539/00/0617-3270 $ 17.50+.50/0

[11] a) O. Mongin, C. Papamicaël, N. Hoyler, A. Gossauer, *J. Org. Chem.* **1998**, *63*, 5568–5580; b) C. C. Mak, N. Bampos, J. K. M. Sanders, *Angew. Chem.* **1998**, *110*, 3169–3172; *Angew. Chem. Int. Ed.* **1998**, *37*, 3020–3023; c) C. C. Mak, D. Pomeranc, M. Montalti, L. Prodi, J. K. M. Sanders, *Chem. Commun.* **1999**, 1083–1084.

[12] a) J. P. Collman, P. Denisevich, Y. Konai, M. Marrocco, C. Koval, F. C. Anson, *J. Am. Chem. Soc.* **1980**, *102*, 6027–6036; b) J. P. Fillers, K. G. Ravichandran, I. Abdalmuhdi, A. Tulinksi, C. K. Chang, *J. Am. Chem. Soc.* **1986**, *108*, 417–424; c) A. Osuka, S. Nakajima, T. Nagata, K. Maruyama, T. Toriumi, *Angew. Chem.* **1991**, *103*, 579–580; *Angew. Chem. Int. Ed. Engl.* **1991**, *30*, 582–584; d) A. Osuka, S. Nakajima, K. Marumaya, *J. Org. Chem.* **1992**, *57*, 7355–7359; e) H. L. Anderson, *Inorg. Chem.* **1994**, *33*, 972–981.

[13] a) D. L. Officer, A. K. Burrell, D. C. W. Reid, *Chem. Commun.* **1996**, 1657–1658; b) N. Kariya, T. Imamura, Y. Sasaki, *Inorg. Chem.* **1997**, *36*, 833–839; c) T. Norsten, N. Branda, *Chem. Commun*. **1998**, 1257–1258; d) L. Ruhlmann, S. Lobstein, M. Gross, A. Giraudeau, *J. Org. Chem.* **1999**, *64*, 1352–1355; e) C. C. Mak, N. Bampos, J. K. M. Sanders, *Chem. Commun*. **1999**, 1085–1089; f) D. Kuciauskas, P. A. Liddell, S. Lin, T. E. Johnson, S. J. Weghorn, J. S. Lindsey, A. L. Moore, T. A. Moore, D. Gust, *J. Am. Chem. Soc.* **1999**, *121*, 8604–8614.

[14] K. Sugiura, H. Tanaka, T. Matsumoto, T. Kawai, Y. Sakata, *Chem. Lett.* **1999**, 1193–1194.

[15] a) J. N. H. Reek, A. P. H. J. Schenning, A. W. Bosman, E. W. Meijier, M. J. Crossley, *Chem. Commun.* **1998**, 11–12; b) L. Jaquinod, O. Siri, R. G. Khoury, K. M. Smith, *Chem. Commun.* **1998**, 1261–1262; c) M. G. H. Vicente, M. T. Cancilla, C. B. Lebrilla, K. M. Smith, *Chem. Commun.* **1998**, 2355–2356; d) K. Sugiura, T. Matsumoto, S. Ohkouchi, Y. Naitoh, T. Kawai, Y. Takai, K. Ushiroda, Y. Sakata, *Chem. Commun.* **1999**, 1957–1958; e) A. Tsuda, A. Nakano, H. Furuta, H. Yamochi, A. Osuka, *Angew. Chem.* **2000**, *112*, 572–575; *Angew. Chem. Int. Ed.* **2000**, *39*, 558–561.

[16] a) O. Mongin, A. Gossauer, *Tetrahedron*, **1997**, *53*, 6835–6846; b) H. A. M. Biemans, A. E. Rowan, A. Verhoeven, P. Vanoppen, L. Latterini, J. Foekema, A. P. H. J. Schenning, E. W. Meijer, F. C. de Schryver, R. J. M. Nolte, *J. Am. Chem. Soc.* **1998**, *120*, 11054–11060.

[17] a) A. Osuka, H. Shimidzu, *Angew. Chem.* **1997**, *109*, 93–95; *Angew. Chem. Int. Ed. Engl.* **1997**, *36*, 135–137; b) N. Yoshida, H. Shimidzu, A. Osuka, *Chem. Lett.* **1998**, 55–56; c) T. Ogawa, Y. Nishimoto, N. Yoshida, N. Ono, A. Osuka, *Chem. Commun.* **1998**, 337–338; d) T. Ogawa, Y. Nishimoto, N. Yoshida, N. Ono, A. Osuka, *Angew. Chem.* **1999**, *111*, 140–142; *Angew. Chem. Int. Ed.* **1999**, *38*, 176–179; e) N. Yoshida, A. Osuka, *Chem. Commun.* **2000**, 197; f) N. Aratani, A. Osuka, Y. H. Kim, D. H. Jeong, D. Kim, *Angew. Chem.* **2000**, *112*, 1517–1521; *Angew. Chem. Int. Ed.* **2000**, *39*, 1458–1462.

[18] *meso*–*meso*-Linked diporphyrins were synthesized independently a) K. Susumu, T. Shimidzu, K. Tanaka, H. Segawa, *Tetrahedron Lett.* **1996**, *37*, 8399–8402; b) R. G. Khoury, L. Jaquinod, K. M. Smith, *Chem. Commun*. **1997**, 1057–1058; c) M. O. Senge, X. Feng, *Tetrahedron Lett.* **1999**, *40*, 4165–4168; d) J. Wojaczynski, L. Latos-Grazynski, P. J. Chmielewski, P. V. Calcar, A. L. Balch, *Inorg. Chem.* **1999**, *38*, 3040–3050; e) X. Shi, L. S. Liebeskind, *J. Org. Chem.* **2000**, *65*, 1665–1671.

[19] For a preliminary report of this work see: A. Nakano, A. Osuka, I. Yamazaki, T. Yamazaki, Y. Nishimura, *Angew. Chem.* **1998**, *110*, 3172–3176; *Angew. Chem. Int. Ed.* **1998**, *37*, 3023–3027.

[20] a) P. N. W. Baxter, J. M. Lehn, A. B. O. Kneisel, D. Fenske, *Angew. Chem.* **1997**, *109*, 2067–2070; *Angew. Chem. Int. Ed. Engl.* **1997**, *36*, 1978–1981; b) E. C. Constable, *Tetrahedron*, **1992**, *48*, 10013–10059.

[21] a) T. Nagata, A. Osuka, K. Maruyama, *J. Am. Chem. Soc.* **1990**, *112*, 3054–3059; b) A. Osuka, T. Nagata, K. Maruyama, *Chem. Lett.* **1991**, 481–484; c) A. Osuka, R.-P. Zhang, K. Maruyama, I. Yamazaki, Y. Nishimura, *Bull. Chem. Soc. Jpn.* **1992**, *65*, 2807–2813.

[22] M. S. Newman, L. F. Lee, *J. Org. Chem.* **1972**, *37*, 4468–4469.

[23] a) Q. M. Wang, D. W. Bruce, *Synlett* **1995**, 1267–1268; b) B. J. Littler, M. A. Miller, C.-H. Hung, R. W. Wagner, D. F. O'Shea, P. D. Boyle, J. S. Lindsey, *J. Org. Chem.* **1999**, *64*, 1391–1396.

[24] a) S. G. DiMagno, V. S.-Y. Lin, M. J. Therien, *J. Org. Chem.* **1993**, *53*, 5983–5993; b) J. S. Lindsey, I. C. Schreiman, H. C. Hsu, P. C. Kearney, A. M. Marguerettaz, *J. Org. Chem.* **1987**, *52*, 827–836; c) B. J. Littler, Y. Ciringh, J. S. Lindsey, *J. Org. Chem.* **1999**, *64*, 2864–2872.

[25] a) K. M. Smith, G. H. Barnett, B. Evans, Z. Martynenko, *J. Am. Chem. Soc.* **1979**, *101*, 5953–5961; b) J. E. Baldwin, M. J. Crossley, J. Debernardis, *Tetrahedron* **1982**, *38*, 685–692.

[26] P. G. Seybold, M. Gouterman, *J. Mol. Spectrosc.* **1969**, *31*, 1–13.

[27] J. L. Sessler, M. R. Johnson, T.-Y. Lin, *Tetrahedron* **1989**, *45*, 4767–4784.

[28] a) I. Yamazaki, N. Tamai, H. Kume, H. Tsuchiya, K. Oba, *Rev. Sci. Instrum.* **1985**, *56*, 1187–1194; b) T. Yamazaki, I. Yamazaki, A. Osuka, *J. Phys. Chem. B* **1998**, *102*, 7858–7865.

Received: April 18, 2000 [F2433]